

PHOTON COUNTING AND ITS
APPLICATION TO MEASUREMENT
OF BIOLOGICAL LUMINESCENCE

A THESIS
SUBMITTED IN PARTIAL FULFILMENT OF
THE REQUIREMENTS FOR THE DEGREE OF
MASTER OF SCIENCE
AT THE
UNIVERSITY OF MANITOBA

BY
A. R. MARTIN
SEPTEMBER, 1952.



PREFACE

The work to be described in this paper
was carried out as part of the research
program at the Manitoba Cancer Relief
and Research Institute under the direction
of Dr. P. A. Macdonald

TABLE OF CONTENTS

	Page
INTRODUCTION	1
SOME PRELIMINARY CONSIDERATIONS	3
Construction and principle of operation of the photomultiplier	3
Sources and magnitude of dark current	4
Background at dry ice temperature	9
DESCRIPTION OF THE APPARATUS	12
Introduction	12
The liquid oxygen container	12
The vacuum system	14
The electronic circuit	15
The monochromator	18
CHARACTERISTICS OF THE APPARATUS	20
Background and selection of photomultipliers	20
Pulse-Height distribution	21
Resolving time of the circuit	22
Efficiency of the detecting system	24
Spectral response of the system	35
APPLICATION TO THE ANALYSIS OF FLUORESCENT SPECTRA	39
CONCLUSIONS	44
REFERENCES	46

INTRODUCTION

The introduction of radiation therapy into the field of medical practice has served to provide a bond of common interest between the medical and physical scientist. Once this contact had been established it became apparent to the physicist that vast groups of biological phenomena awaited investigation by physical methods, and that medical investigations could well have been carried out in some of the older fields of physics many years ago. This is particularly true of the field of spectroscopy.

The present thesis was prepared in a spectroscopic laboratory investigating various biological phenomena, amongst which were the absorption spectra of biologically active compounds. These studies naturally led to tracing the path of the selectively absorbed energy, which in turn necessitated the examination of the fluorescent spectra of the compounds concerned. Specifically, in relation to this thesis, the work of Macdonald and Margolese⁽¹⁾ has established that female sex tissue fluoresces under ultra-violet light to yield spectra that can be immediately associated with the physiological condition of the individual under study. Subsequent to the above publication, further work in the same laboratory has established the conditions under which the biochemical compounds present in the sex tissue might be made to fluoresce in vitro.

This development offers the possibility of utilizing quantitative spectrophotometry of fluorescent tissue as a method of directly estimating the concentration of various sex hormones in the female system. In order to complete the link between the laboratory measurements of these fluorescent compounds and the fluorescence in the tissue itself, it becomes necessary to make quantitative measurements of the emission spectra of the tissue excited under ultra-violet radiation.

Since the intensities of the emitted spectra are very low and the measurements must be made rapidly, this spectral analysis requires the development of a highly sensitive detecting system for use in conjunction with a monochromator.

The utilization of photomultiplier tubes, coupled with modern electronic counting circuits to measure light of very low intensity obviously suggests itself and it is this specific problem that constitutes the subject matter of the present paper.

SOME PRELIMINARY CONSIDERATIONS

CONSTRUCTION AND PRINCIPLE OF OPERATION OF THE PHOTOMULTIPLIER

In order to appreciate more fully the problem at hand, it is desirable to examine briefly the construction and principle of operation of the photomultiplier. This instrument consists of a photocathode and a number of secondary emission surfaces, (dynodes) enclosed in an evacuated envelope. The envelope, in commercial types at least, is generally of glass selected with due regard to the required spectral transmission. The dynode stages are maintained at voltages which increase positively from the cathode in steps of from 50 to 200 volts, depending on the type of multiplier used. An electron liberated from the photocathode is accelerated to the first dynode where it releases, on the average, three or four secondary electrons, which in turn are accelerated to the second dynode. This multiplicative process continues through all the stages, electrons from the final stage being collected at the anode. A nine-stage commercial multiplier, such as type 931A, operating at 80 volts per stage, has a multiplication factor of about 3 at each dynode. The overall current amplification in this case then, is 3^9 or approximately 2×10^4 . Higher stage voltages increase the secondary emission ratio yielding an overall gain of as high as 10^5 in a nine-stage tube at 100 volts per stage.

To obtain high efficiencies, it is necessary that the electrons leaving the dynode stages be guided to the succeeding ones without loss. This is accomplished in the 931A type of

multiplier by shaping the dynodes to provide the correct electrostatic focusing. These dynodes are arranged in a circular array for compactness, but similar focusing action may be obtained with a linear arrangement. Other multipliers employ a succession of screen dynodes separated by glass rings which become negatively charged and prevent the drift of electrons toward the periphery of the tube. Magnetic focusing, employed earlier in the development of the photomultiplier, is now rarely resorted to, largely because of the bulk and inconvenience of the auxiliary apparatus. (2)

SOURCES AND MAGNITUDE OF DARK CURRENT

The primary consideration in the application of the photomultiplier to low light levels is the anode dark current of the tube. This has been discussed fully by Engstrom, with regard to the 931A and 1P21, (3) and is attributed to two major sources: 1) ohmic leakage; 2) amplified thermionic emission. A third source, regenerative ionization, becomes dominant in this type of tube at about 110 volts per stage, and may be avoided by working below this voltage level. Ohmic leakage, which is proportional to the applied voltage, dominates up to about 80 volts per stage, above which it is surpassed in magnitude by the amplified thermionic emission. The latter, being proportional to the gain of the tube, varies in this region approximately as the fifth power of the voltage. In an average 931A at 100 volts per stage, operating at room temperature, the total magnitude of the dark current is of the

order of 10^{-7} amperes, about 10 per cent of which is due to ohmic leakage. Considerable variations in these values may be expected from tube to tube.

Thermionic emission may be reduced by two means:

1) by cooling the emitting surfaces; and 2) by lowering the applied voltage. The thermionic emission from the cathode at room temperature may be estimated by using Richardson's equation:

$$j = AT^2 e^{-\frac{\phi}{kT}} = AT^2 e^{-\frac{11,607 \phi}{T}}$$

where j = thermionic emission in amperes/cm²

A = a constant depending on the surface material

ϕ = the work function of the material, in volts

T = the temperature of the emitter in absolute degrees.

For the caesium-antimony surface of the 931A cathode ϕ will be approximately one volt, and A about 0.1 amperes per square centimeter. The thermionic emission from the cathode at room temperature, then, will be of the order of 1.5×10^{-13} amperes per square centimeter, or a total of about 5×10^{-13} amperes. If the tube is operated at 90 volts per stage, the overall gain is approximately 5×10^5 , yielding an anode current, due to thermionic emission from the cathode, of 2.5×10^{-7} amperes.

At dry ice temperature ($\sim 235^{\circ}\text{K.}$), this is reduced to about 3.5×10^{-12} amperes, and at liquid oxygen temperature ($\sim 100^{\circ}\text{K.}$) to 6.5×10^{-42} amperes.

It may be expected then, that for all practical purposes, thermionic emission may be completely eliminated by operating the multiplier at liquid oxygen temperature.

The above calculation, however, ignores a field emission effect which is undoubtedly present, due to the potential of the first dynode. In the absence of an external field, the potential barrier at the cathode surface is roughly of the form indicated in Figure 1(a) and, as the calculations indicate, the electrons within the surface have, at low temperatures, an extremely small probability of attaining enough energy to escape. The presence of an external electrostatic field alters this situation by changing the shape of the barrier as indicated in Figure 1(b). An electron having insufficient energy to escape over the barrier now has a finite probability of penetrating it and escaping from the surface.

Engstrom has demonstrated that this effect contributes to the so-called thermionic dark current,⁽⁴⁾ so that the

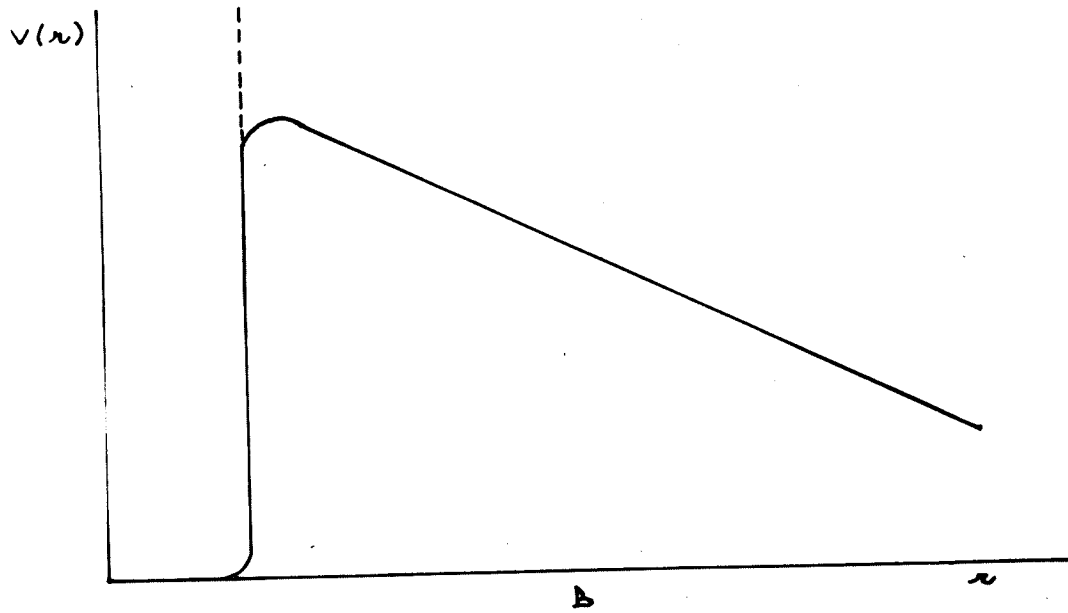
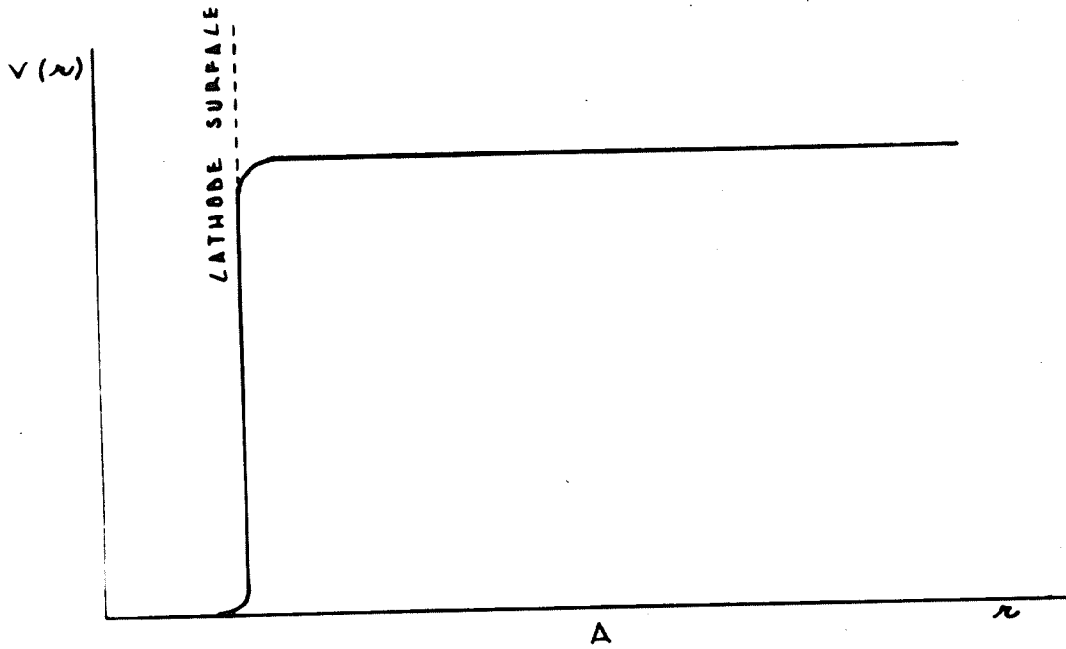


FIGURE 1
 POTENTIAL BARRIER FOR AN ELECTRON
 IN A METAL
 A- NO EXTERNAL FIELD
 B- STRONG EXTERNAL ELECTROSTATIC FIELD

emission from the cathode at liquid oxygen temperature, though small in magnitude, is not completely absent. The net effect is similar to that of lowering the height of the potential barrier, so that in addition to increasing the dark current, the external field will increase the photoelectric efficiency of the cathode. Consequently any attempt at reducing the field emission by lowering the potential of the first dynode will result in a corresponding reduction in photoelectric sensitivity. In actual operation, a compromise must be reached between minimum background and maximum sensitivity.

While this discussion has dealt solely with emission from the cathode, similar considerations apply to the dynodes. However, these elements will contribute to the thermionic dark current to a lesser degree for two reasons: 1) electrons originating at the dynodes undergo less multiplication before reaching the anode; and 2) the dynode work function is higher, resulting in reduced thermionic emission. There is little to be gained by operating at low inter-dynode voltages since the only significant effect is to reduce the overall gain of the tube, leaving the signal-to-noise ratio unchanged.

Whereas the background due to thermionic emission may be controlled by refrigeration as indicated above, very little can be done to reduce the ohmic leakage. An attempt was made to minimize this leakage by stripping the base from a 1P21 and carefully cleaning the glass envelope, but this procedure

yielded no perceptible improvement. It was concluded that the ohmic leakage was almost entirely due to poor insulation in the interior of the tube.

The anode dark current of several 1P21 and 1P28 photomultipliers was measured at room temperature by enclosing the tube in a light tight brass cylinder and connecting a galvanometer of 10^{-9} amperes per millimeter sensitivity between the collector and high tension supply. The appropriate dynode voltages were supplied by connecting a bleeder of ten 270K resistors between the pins of the tube socket. At 90 volts per stage the background varied from tube to tube between 10^{-7} and 10^{-6} amperes as expected. One multiplier however, (a 1P21) had an anode dark current of only 8×10^{-9} amperes. This indicated not only good interior insulation, but also either extremely low thermionic emission or unusually low gain. Thermionic emission of this magnitude could be accounted for by assuming a work function of about 1.08 volts. This would reduce the emission from the cathode at 235°K. from 7×10^{-18} amperes (2700 electrons per minute) as previously calculated, to about 10^{-19} amperes, or 37 electrons per minute. There was, then, a possibility that an adequate reduction in thermionic background could be obtained by operating the multiplier at dry ice temperature, and it was decided to investigate the performance of the tube at this temperature before proceeding with the more complicated and expensive problem of refrigeration with liquid oxygen.

BACKGROUND AT DRY ICE TEMPERATURE

The container illustrated in Figure 2 was constructed for the purpose of cooling the tube with dry ice, the inner cylinder being evacuated to about 50 microns pressure with a Central Scientific Company "Hypervac" mechanical pump to prevent condensation of moisture around the electrical terminals. In order that the cathode temperature might be estimated, a small coil of number 30 copper wire was wound on the cathode pin of the photomultiplier and connected in one arm of a Wheatstone bridge. Its resistance at room temperature (31.7°C .), was determined and the graph of Figure 3 drawn, using the known temperature coefficient of resistance of copper.

Both a galvanometer and a pulse-counting system were employed in measuring the background of the LP21. The galvanometer previously mentioned was connected in the anode circuit and simultaneous readings of anode current and temperature taken as the tube cooled. The resulting graph is plotted in Figure 5, and shows a minimum current of 2.3×10^{-9} amperes at -39°C .

This procedure was then repeated using the pulse-counting system. The galvanometer was replaced by a 0.5 megohm anode resistor, pulses developed across this resistor being fed through a cathode-follower and linear amplifier into a scale of 64 and mechanical register. (The circuit components are identical with those used later in this project and will be described

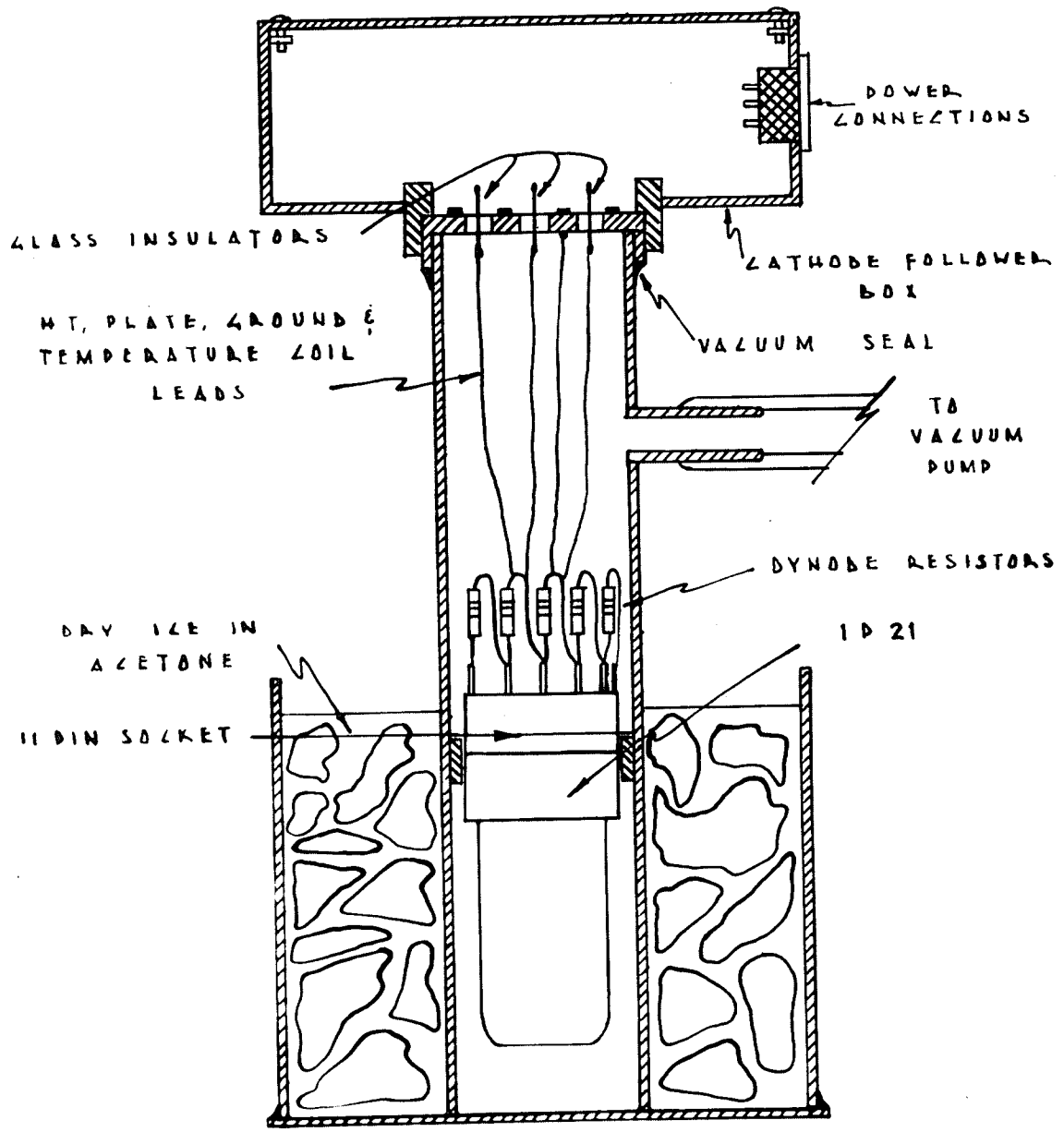


FIGURE 2
 CONTAINER FOR
 PHOTOMULTIPLIER COOLING

subsequently in some detail.) Adjustable pulse-height discrimination was provided on the input circuit of the amplifier, allowing the selection of any one of 30 discrimination levels between 1 and 100 millivolts.

A rough estimate of the expected average background pulse-height may be obtained if the pulse is assumed to be a square-wave and the circuit time-constants such that its width is of the order of 10^{-5} seconds. A pulse originated by a single electron leaving the cathode will, on arrival at the anode consist of approximately 10^5 electrons (if the tube is operated at 90 - 100 volts per stage), or a charge of the order of 2×10^{-14} coulombs. The instantaneous value of the current then, subject to the above assumptions, will be 2×10^{-9} amperes, yielding a voltage drop of 10^{-3} volts across the 0.5 megohm anode resistor. The cathode follower gain was about 0.8 so that this would result in a pulse of slightly less than a millivolt arriving at the amplifier input.

However, the counting rate of the system was limited by the mechanical register to about 40,000 counts per minute, requiring, at 90 volts per stage, a discrimination level of 10^{-3} volts to prevent jamming at room temperature. The data plotted in Figure 4 were obtained while operating at this level.

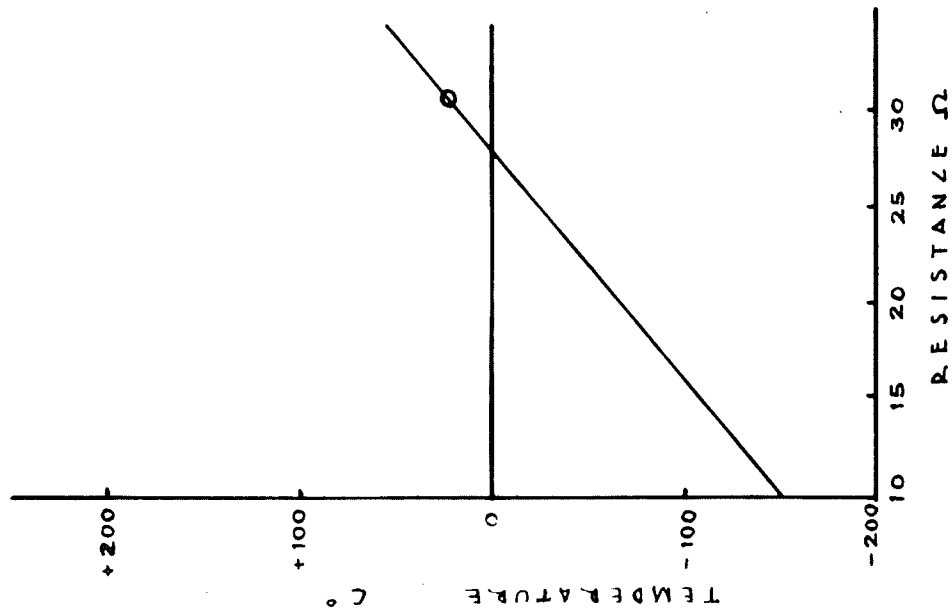


FIGURE 3
CALIBRATION
OF TEMPERATURE
MEASURING COIL

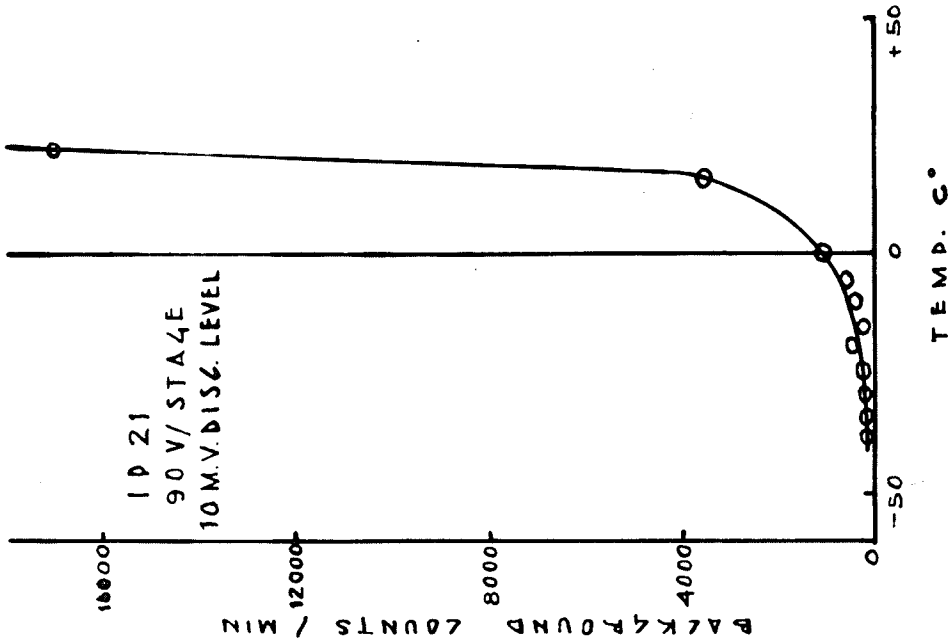


FIGURE 4
VARIATION
OF BACKGROUND
WITH TEMPERATURE

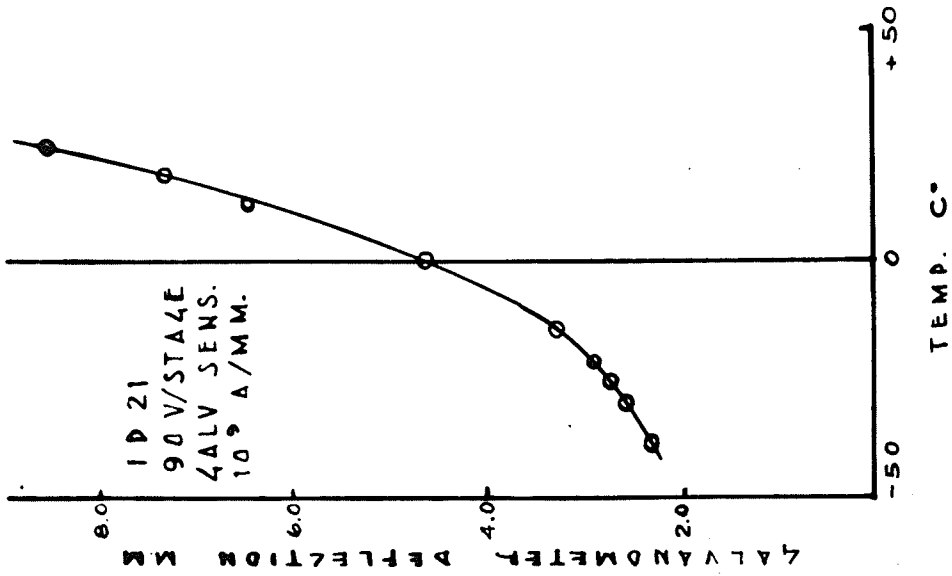


FIGURE 5
VARIATION OF
ANODE CURRENT
WITH TEMPERATURE

The temperature plotted in Figures 4 and 5 are, of course, those of the cathode pin on the base of the multiplier, not the actual cathode temperatures. Whereas the resistance coil reached a constant temperature in about $1\frac{1}{2}$ hours, it was over two hours before the background pulse-count reached a stable value. During this additional half-hour required by the cathode to reach an equilibrium temperature, the background dropped from 115 counts per minute, as indicated in Figure 5, to 76 counts per minute. No such lag was observable on the galvanometer scale.

The background count at -39°C . and a 1 millivolt discrimination level was 1100 pulses per minute — considerably higher than anticipated. It was concluded that for maximum sensitivity it would be necessary to operate the photomultiplier at liquid oxygen temperature.

DESCRIPTION OF THE APPARATUS

INTRODUCTION

The apparatus was built around a 1P21 housed in a container holding liquid oxygen, this container being placed so that the light from the output slit of the monochromator passed through a window in the outer wall to the cathode of the photomultiplier. The resulting pulses, developed across the anode resistor of the 1P21, were fed through a cathode follower and linear amplifier to the scaling unit. A high vacuum was required in part of the container so that a vacuum system also had to be assembled.

The apparatus will be discussed in detail under the following headings: 1) the liquid oxygen container; 2) the vacuum system; 3) the electronic circuit; and 4) the monochromator.

THE LIQUID OXYGEN CONTAINER

The main difficulties accompanying refrigeration with liquid oxygen are: 1) condensation of moisture, causing leakage between electrical contacts, and fogging of light-admitting windows; 2) the rapid rate of evaporation of the liquid. After surveying the available literature on the subject, it was decided that a modification of a container described by R. W. Engstrom⁽⁵⁾ would be most suitable in overcoming these problems. This

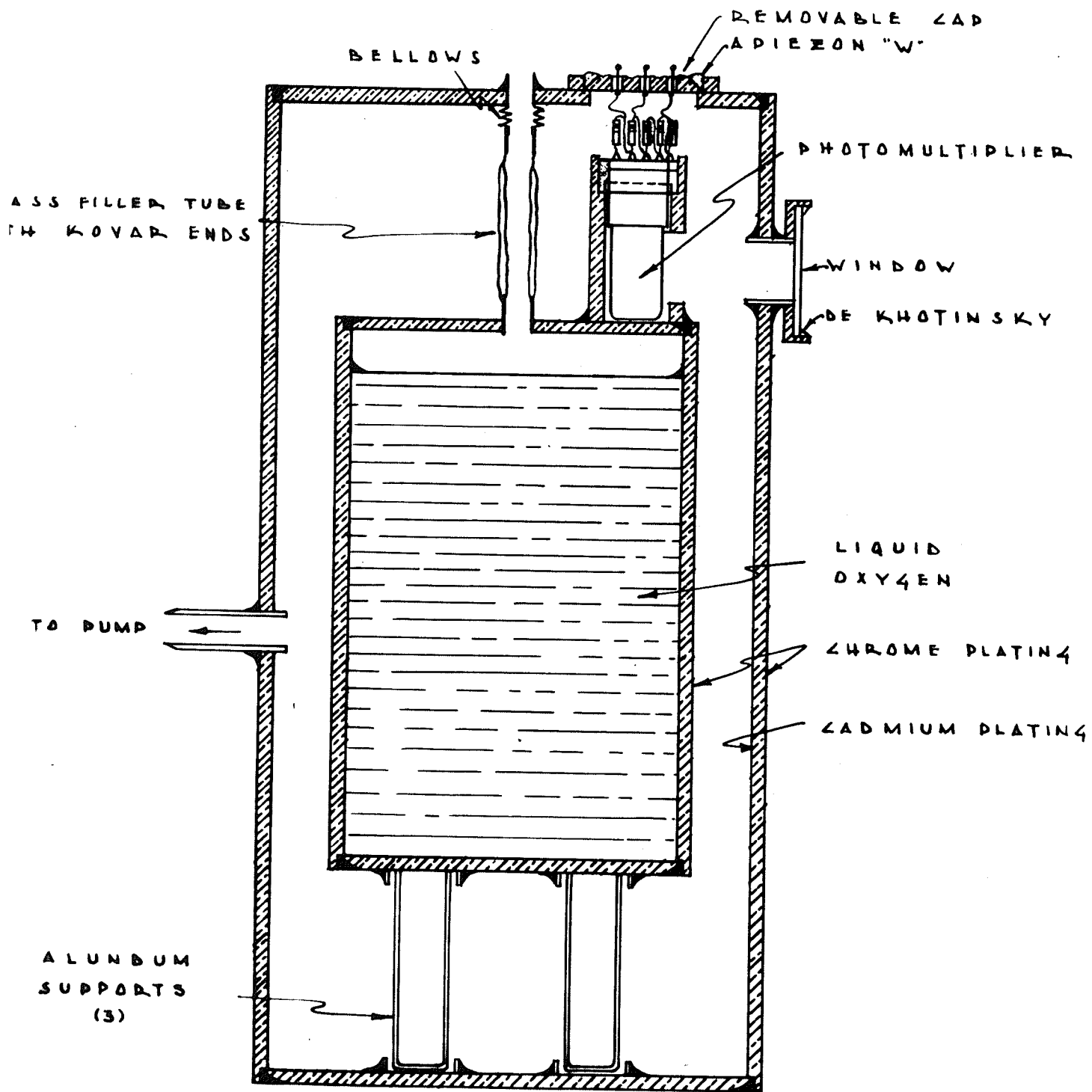


FIGURE 6.
LIQUID OXYGEN
CONTAINER

container, illustrated in Figure 6, consisted of a small cylindrical tank of four litres capacity, supported inside a larger canister on three insulating legs. The space between the tanks was evacuated, the inner one being accessible for filling with oxygen through a large diameter glass tube. The photomultiplier was supported by its base in a heavy brass sleeve on top of the inner container, light being admitted to the cathode through a circular window consisting of a plane flashlight glass sealed in the outer wall with DeKhotinsky cement.

Brass was used throughout the construction except for the cylindrical wall of the outer tank which was 9" I.D. steel pipe. All seams were soft-soldered. The outsides of both tanks were chromium plated, and the inside of the larger one cadmium plated to reduce the exchange of heat by radiation. This work was done by Winnipeg Brass Ltd. The use of cadmium plate was necessitated by the fact that the bottom of the outside tank was soldered in place before the plating operation, rendering it impossible to do an adequate plating job with chromium.

The inner tank was supported by Alundum thimbles, nine centimeters in length, chosen because of the low thermal conductivity of the material (about 3×10^{-4} c.g.s. units as compared to 2×10^{-3} c.g.s. units for glass.) There are other materials, of course, such as paraffin, beeswax or masonite, that have equal or better insulating properties, but their relatively low strengths require the use of larger volumes of material, resulting in greater thermal losses.

The filler tube, obtained commercially, was of Pyrex with Kovar ends. The lower end was soft-soldered into the top of the inner container, and the upper end to a small steel bellows. This bellows, which was then soldered into the top of the outer tank, served to relieve the filler tube of any strain due to the contraction of the inner tank when reduced to liquid oxygen temperature. It was estimated that this contraction would be of the order of one millimeter. Light was prevented from reaching the multiplier through the glass tube by plugging the filler hole with a rubber stopper. A two-foot length of small black rubber tubing pushed into a hole in the stopper allowed evaporating oxygen to escape without admitting light:

Access to the multiplier was provided by a small lid sealed in the top of the outer tank with Apiezon "W". Electrical leads were taken through pyrex beads sealed in the lid. These beads, a commercial product, are provided with a Kovar rim and centre stem. The rims were soft-soldered directly to the lid, providing a trouble-free vacuum seal.

THE VACUUM SYSTEM

The vacuum was maintained between the walls of the containers by means of a mechanical pump (Central Scientific Company "Hypervac" vacuum pump) in series with an oil diffusion booster pump (Distillation Products model MB 727).⁽⁶⁾ Connections

between the units were made with brass tubing coupled with rubber hose. All joints were painted liberally with red glyptal.

While it was not considered necessary to include a vacuum gauge in the system, it was estimated from the rate of evaporation of the liquid oxygen that the vacuum obtained was of the order of 10 microns or better. (*) Four litres of liquid oxygen lasted from 36 to 48 hours. Leaks were readily detected as they immediately resulted in sparking between the high-tension terminals on the tube base. This is due to a variation in sparking potential with pressure. If we consider two electrodes placed a fixed distance apart in air, and suppose that the pressure of the air is slowly reduced, then the sparking potential between them slowly decreases until it reaches a minimum value. This minimum depends, of course, on the shape and spacing of the electrodes. As the pressure is reduced further, the sparking potential rises quite rapidly. In the case under consideration, the pressure was below the point of minimum sparking potential, so that a slight increase in pressure due to a leak in the system reduced the sparking potential, causing a discharge between the high-tension terminals.

THE ELECTRONIC CIRCUIT

The electronic circuit is shown schematically in Figure 7, and may be subdivided, for purposes of discussion, into three units: 1) the photomultiplier and cathode follower;

* see reference (5)

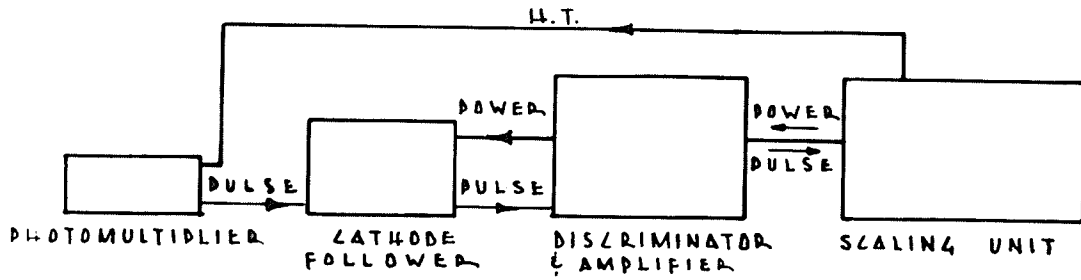


FIGURE 7
SCHEMATIC CIRCUIT

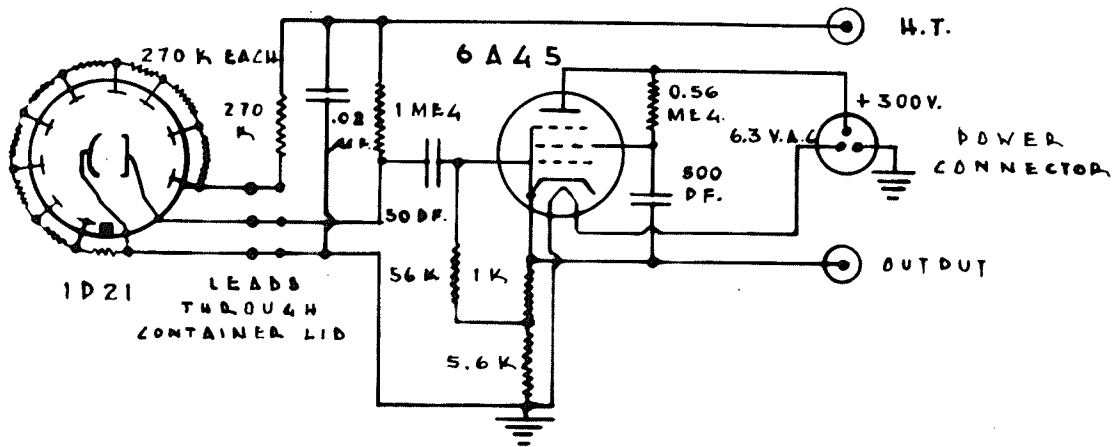


FIGURE 8
PHOTOMULTIPLIER
& CATHODE FOLLOWER CIRCUIT

2) the linear amplifier; and 3) the scaling unit.

The photomultiplier and cathode follower circuit is illustrated in Figure 8. The high tension supply was taken from the H. T. generator in the scaler through a co-axial cable to the cathode follower box, and thence to a bleeder of ten 270K resistors connected between the dynodes. The resistors around the base of the multiplier socket increased to about 320K each at liquid air temperature so that the voltage between the last dynode and the collector was slightly less than the remaining inter-dynode voltages. Since there is no multiplication at the collector, this has no adverse effect on the performance of the tube.

Pulses developed across the one megohm anode resistor were fed through a 50 pf. condenser to the control grid of the cathode follower. The plate and filament supply for the 6AG5 were obtained from the scaler power supply through the amplifier. The circuit components indicated yielded an anode current of approximately three milliamperes with an anode voltage of 290 volts and the screen grid dropping resistor placed the screen at about 240 volts, the screen current being about 0.8 milliamperes. The cathode was positive with respect to ground by 25.6 volts and the screen grid biased negatively with respect to the cathode by 3.8 volts. Plots of the static transfer and plate characteristics in the region of operation indicated a plate resistance, R_p , of approximately 0.8 megs., and a transconductance, g_m of the order of 1200 micromhos. From

these values the following were calculated:

$$\begin{aligned} \text{Tube amplification:} \quad \mu &= g_m R_p = 960 \\ \text{Output impedance:} \quad Z_o &\approx \frac{1}{g_m} \approx 835 \Omega \\ \text{Voltage amplification:} \quad \frac{E_o}{E_i} &= \frac{\mu R_c}{(\mu+1)R_c + R_p} \approx 0.89 \end{aligned}$$

where R_c = cathode bias resistor
= 6.6 K.

The cathode follower was enclosed in a light-tight box designed to fit over the lid of the liquid oxygen container, thereby preventing stray light from reaching the multiplier through the pyrex beads. The 6AG5 was carefully wrapped with "Scotch" electrical tape to prevent the escape of illumination from the filament.

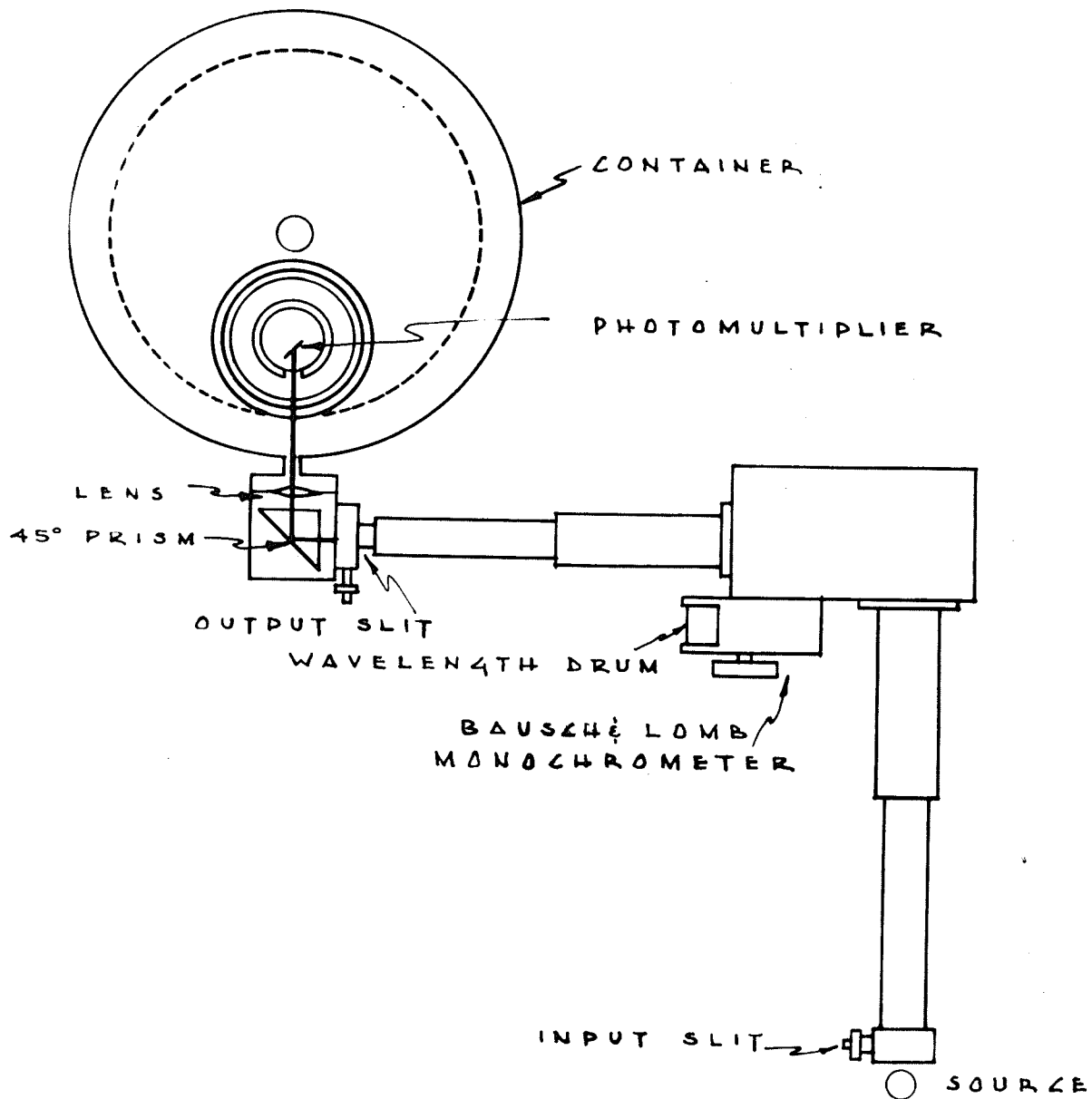
The linear amplifier (Nuclear Instrument and Chemical Company Model 1061) was designed for operation from the scaler power supply (150 and 300 v.d.c., 6.3 v.a.c.). A 3-pin output plug was added to the amplifier to carry the 6.3 v. and 300 v. supplies on to the cathode follower. The pulses from the 6AG5 cathode were carried by a co-axial cable to a cathode-follower input circuit in the amplifier having a measured time constant of about 5 microseconds. Adjustable pulse-height discrimination from 1 to 100 millivolts was provided by an attenuator in the cathode circuit. The amplifier consisted of two 2-stage feedback loops with an overall gain of about 400, feeding into a

monostable multivibrator output circuit. The overall resolving time was claimed to be better than 5 microseconds.

The scaling unit (Nuclear Instrument and Chemical Company Model 161) was originally designed for use with a Geiger counting tube, and required a few minor circuit changes to facilitate interconnection with the other units. Pulses from the amplifier were fed into a discriminator input circuit adjusted to a 0.3 volt level, and passed on to a Higginbotham scale of 64 and mechanical register. The low scaling factor made high-speed counting impossible as counts were lost in the mechanical register at rates greater than about forty thousand per minute. The high tension generator in the unit had an output variable between 500 and 1500 volts.

THE MONOCHROMATOR

Light passing into the photomultiplier was first analyzed by a Bausch and Lomb monochromator connected to the window of the container as illustrated in Figure 9. The monochromator was a constant deviation type employing a Pellin-Broca prism on a rotating table connected to a calibrated wavelength drum reading from 4000 to 8000 Angstroms. Light from the output slit was reflected at right angles by a 45° prism and focussed on the multiplier cathode by a convex lens of suitable focal length. The resultant relative positions of the monochromator and container made the wavelength drum easily accessible for reading.



. FIGURE 9 .
 . MONOCHROMATOR .
 . & LIQUID OXYGEN CONTAINER .

The monochromator constants as supplied by the manufacturer are as follows:

Prism index of refraction: ($\lambda = 5893 \text{ \AA}$)	1.7201
Base of equivalent 60° prism:	35.5 mm.
Focal lengths of collimator and telescope objectives:	284.4 mm.
Diameter of collimator and telescope objectives:	31.0 mm.

Since the focal lengths of the collimator and telescope are equal, the magnification of the input slit image is unity and the slits should be kept at equal widths. The normal slit widths for $\lambda = 4000 \text{ \AA}$ and 5893 \AA respectively are .0016 mm. and .0023 mm. Graphs of resolving power as a function of slit width for these two wavelengths are shown in Figure 10.

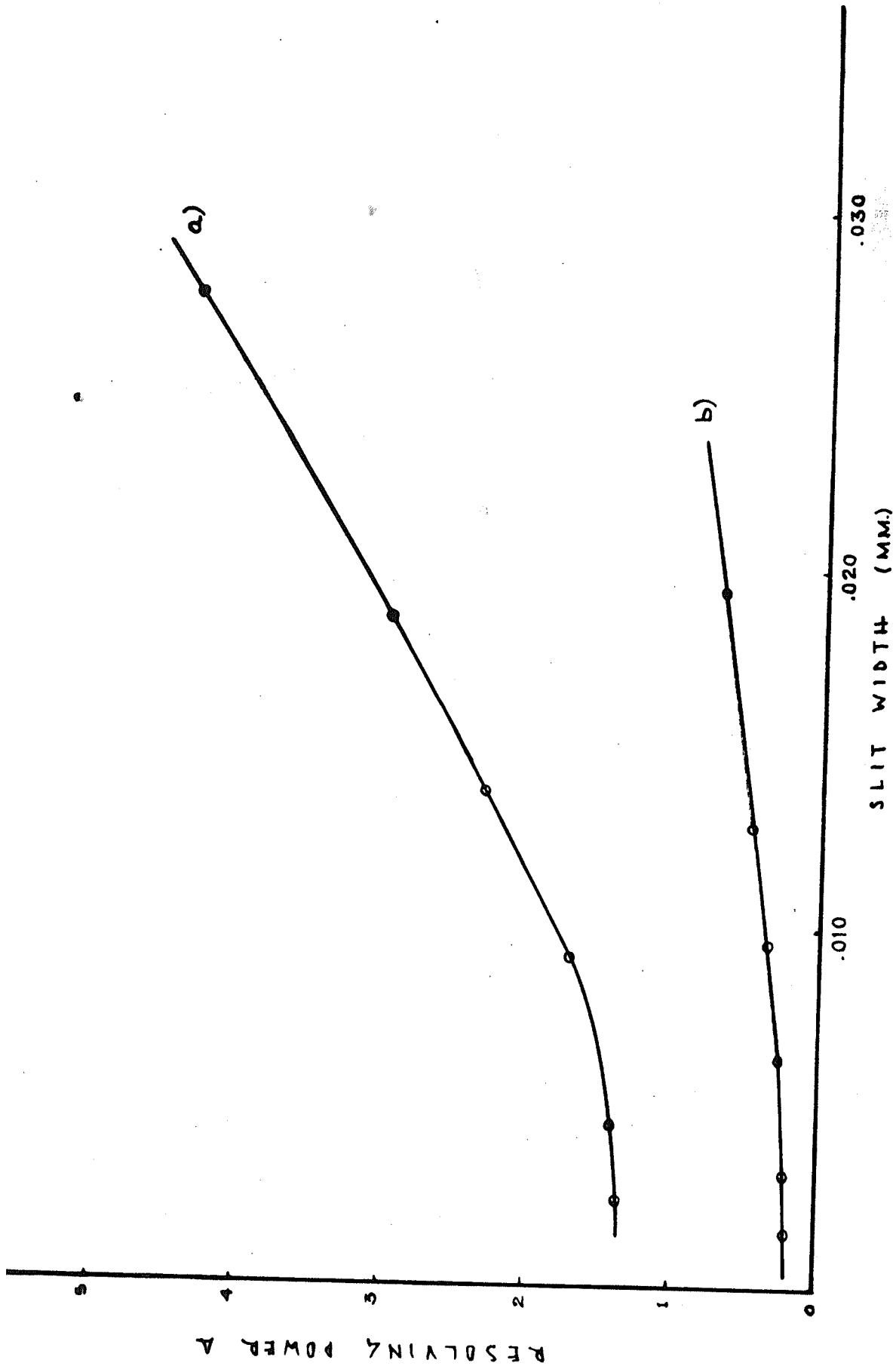


FIGURE 10
 RESOLVING POWER OF MONOCHROMATOR
 AS A FUNCTION OF SLIT WIDTH
 AT a) 5893 Å b) 4000 Å

CHARACTERISTICS OF THE APPARATUS

BACKGROUND AND SELECTION OF PHOTOMULTIPLIERS

After four hours in the liquid oxygen container, the background of the original 1P21 used was reduced to 48 pulses per minute at a one millivolt discrimination level. Unfortunately this tube developed a crack in the envelop and had to be replaced. Nine new multipliers (four 1P21, two 1P28 and three 931A) were tested for background, and one, a 931A, was found to have a background of only 38 pulses per minute at liquid oxygen temperature and 1 millivolt discrimination level. The remainder had backgrounds between this value and 50,000 pulses per minute. This 931A subsequently proved more sensitive than the 1P21 previously employed, and was used for the remainder of the work.

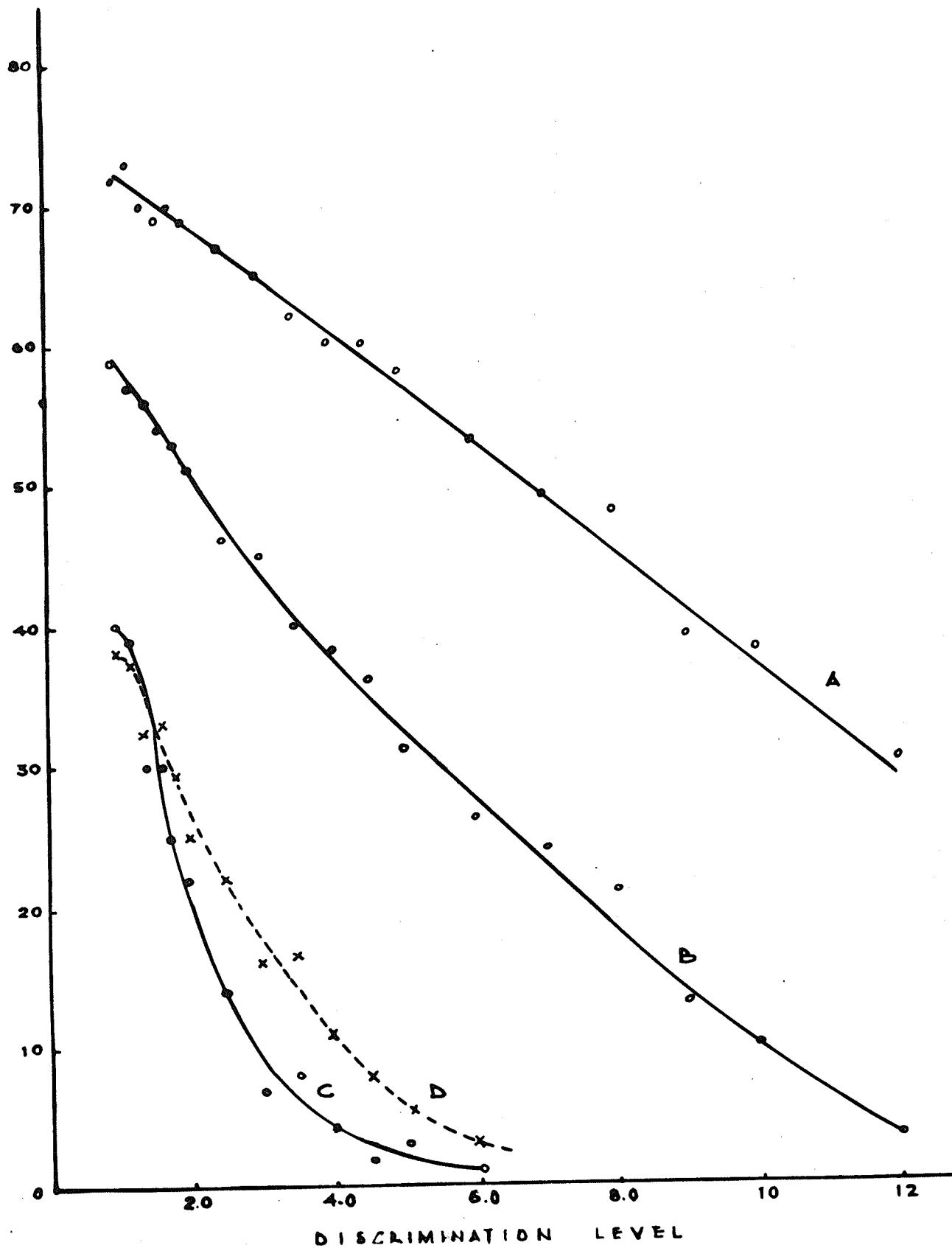
It was found, as noted in a previous investigation by Blanc-Lapierre and Charles⁽⁷⁾ that a multiplier with excessively high background at room temperature was not much improved by cooling. It is likely that in this case the high background is largely due to excessive ohmic leakage. In general the background measured with a 25 millivolt discrimination level at room temperature gives a fair indication of the background above 1 millivolt to be expected at liquid oxygen temperature.

PULSE-HEIGHT DISTRIBUTION

In order to determine the best multiplier voltage and discrimination level to employ, the pulse-height distribution was measured for both background pulses and those due to a weak light signal. Figure 11 is a plot of background against discrimination level for the 1P21 at 75, 90 and 100 volts per stage, and the 931A at 100 volts per stage. Results obtained with a weak signal (background subtracted) under the same conditions are plotted similarly in Figure 12. It may be noted from the graphs that the 931A at 100 volts per stage and a 1 millivolt discrimination level displayed a higher sensitivity and lower background than the 1P21 operating under similar conditions.

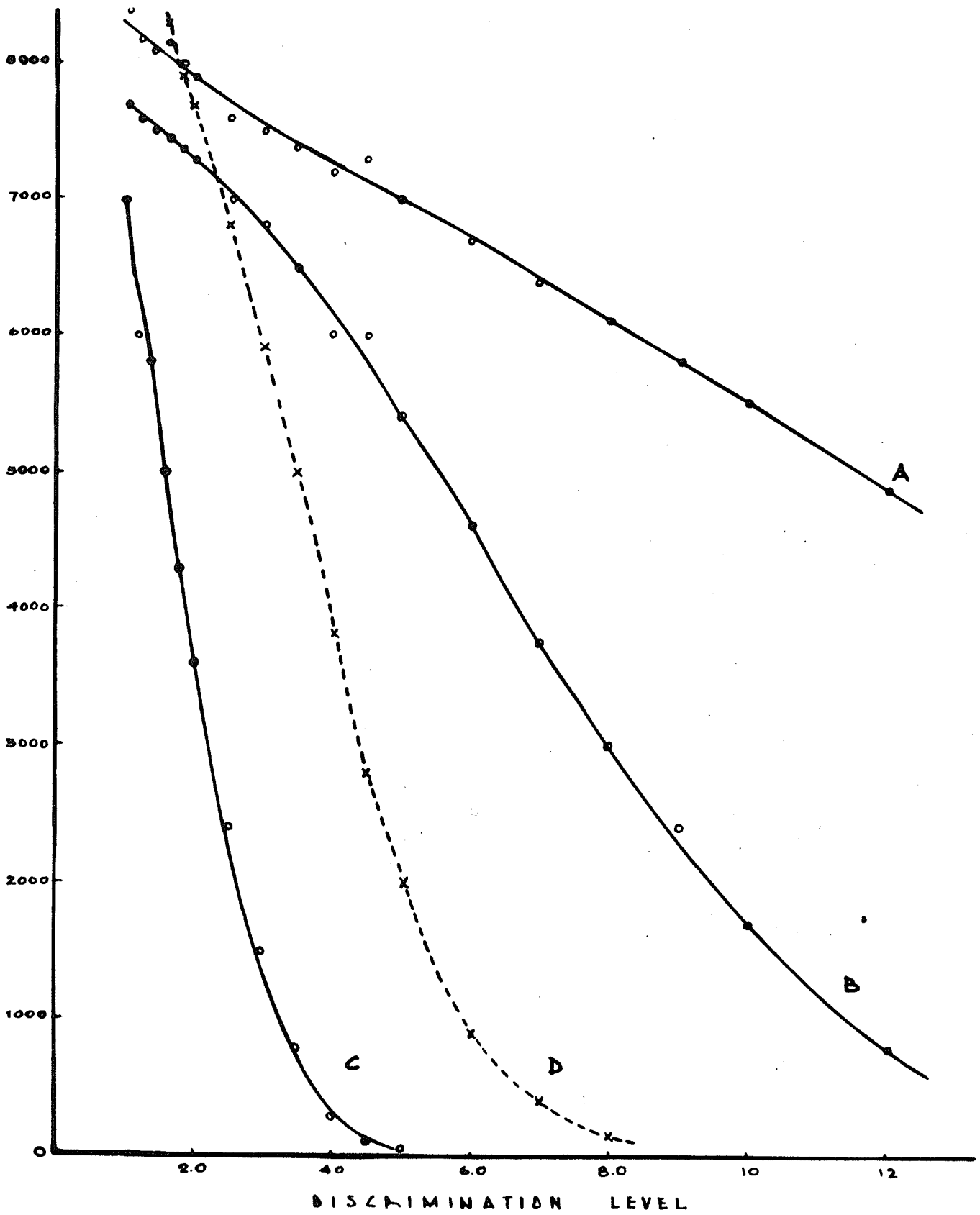
Table 1 is obtained directly from curves D of Figures 11 and 12 and indicates the number of pulses per minute falling in the intervals between adjacent discrimination levels. Table 2 is obtained from Table 1 by dividing these values by the width of the interval concerned (expressed in tenth-millivolts), and gives the approximate number of pulses per minute falling in a tenth millivolt range in the middle of each interval. The values from this Table are plotted in Figure 13. The curves so obtained are the background and signal pulse-height distribution curves for the 931A at liquid oxygen temperature.

There is a characteristic difference between the distributions of background and signal pulse-heights due to the fact that background pulses may originate at the dynodes as well as at the



1D 21 100 V/ STAGE
 1D 21 90 V/ STAGE
 1D 21 75 V/ STAGE
 931A 100 V/ STAGE

FIGURE 11
 BACKGROUND
 PULSE HEIGHT DISTRIBUTION



A 1P21 100 V/ STAGE
 B 1P21 90 V/ STAGE
 C 1P21 75 V/ STAGE
 D 931A 100 V/ STAGE

FIGURE 12
 SIGNAL PULSE-HEIGHT
 DISTRIBUTION

TABLE I

INTERVAL	COUNTS/MINUTE	
	Background (Fig. 11 D)	Signal (Fig. 12 D)
1.0 - 1.2 millivolts	1.0	--
1.2 - 1.4 "	2.4	--
1.4 - 1.6 "	2.6	--
1.6 - 1.8 "	3.0	320
1.8 - 2.0 "	2.6	340
2.0 - 2.5 "	5.2	900
2.5 - 3.0 "	4.0	920
3.0 - 3.5 "	3.6	1000
3.5 - 4.0 "	3.0	1040
4.0 - 4.5 "	--	1000
4.5 - 5.0 "	--	800
5.0 - 6.0 "	--	1120
6.0 - 7.0 "	--	480
7.0 - 8.0 "	--	240

TABLE II

INTERVAL	COUNTS/MINUTE	
	Background	Signal
1.05 - 1.15 millivolts	0.5	-
1.25 - 1.35 "	1.2	-
1.45 - 1.55 "	1.3	-
1.65 - 1.75 "	1.5	160
1.85 - 1.95 "	1.3	170
2.2 - 2.3 "	1.0	180
2.7 - 2.8 "	0.8	184
3.2 - 3.3 "	0.7	200
3.7 - 3.8 "	0.7	208
4.2 - 4.3 "	-	200
4.7 - 4.8 "	-	160
5.45 - 5.55 "	-	112
6.45 - 6.55 "	-	48
7.45 - 7.55 "	-	24

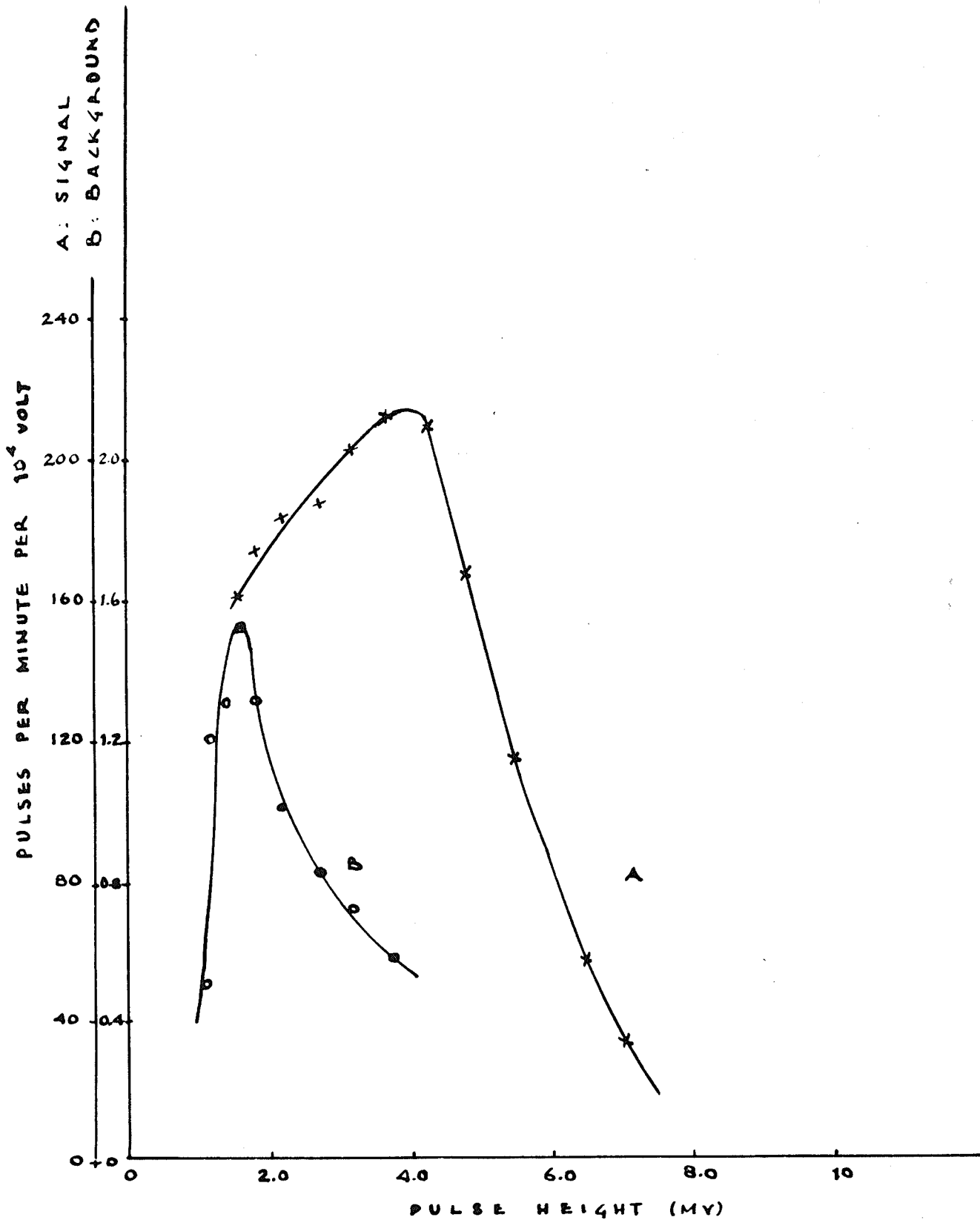


FIGURE 13
 PULSE HEIGHT DISTRIBUTION
 931 A 100 V/STAGE
 A - WEAK SIGNAL B - BACKGROUND

cathode. Advantage may be taken of this, in tubes with high background, by discriminating at an appropriate level, thereby gaining an increased signal-to-noise ratio without excessive loss of sensitivity.

RESOLVING TIME OF THE CIRCUIT

The resolving time of the counting circuit was found by a method similar to that used with Gieger counting systems, utilizing the double light source illustrated in Figure 14. This source consisted of two 1.6 volt flashlight bulbs, each mounted behind a pair of pinhole apertures. The two collimated beams of light thus produced fell on the photomultiplier cathode about half an inch apart. Intercepting both beams between the first and second pinholes were a pair of polaroid lenses, one fixed, the other free to rotate. A scale graduated from zero to ninety degrees, engraved on the rim of the movable polaroid, indicated the relative orientation of the axes. The bulbs were each connected in series with a 100 ohm "Heliopot" rheostat and a milliammeter to a parallel combination of six number 6 dry cells. The rheostats, together with the polaroids, provided a reasonably critical adjustment of the intensity of illumination falling on the photomultiplier cathode from each lamp.

Now suppose the polaroids and filament currents have been adjusted so that each lamp yields a convenient counting rate, and lamp "A" is turned on. This will result in say N_1

photons per second arriving at the cathode and producing observable pulses. If only n_1 of these are registered by the system which has a resolving time t , then the total dead time per second is given by $n_1 t$ and the number of counts arriving during this dead period will be $N_1 n_1 t$. Then:

$$N_1 - n_1 = N_1 n_1 t$$

$$\text{or } N_1 = \frac{n_1}{1 - n_1 t} \quad \text{--- (1)}$$

More strictly, this equation should be written:

$$N_1 + B = \frac{n_1 + B}{1 - (n_1 + B)t} \quad \text{where } B \text{ is the background.}$$

However, if we arrange that $n_1 \gg B$, then equation (1) will be sufficiently accurate.

If lamp "B" is now turned on also, producing N_2 additional pulses per second, then:

$$N_1 + N_2 = \frac{n_{12}}{1 - n_{12}t} \quad \text{--- (2)}$$

where n_{12} is the observed counting rate. On extinguishing lamp "A" this counting rate will be reduced to say n_2 pulses per second, and:

$$N_2 = \frac{n_2}{1 - n_2 t} \quad \text{--- (3)}$$

Combining equation (1), (2) and (3) yields:

$$\frac{n_{12}}{1 - n_{12}t} - \frac{n_1}{1 - n_1 t} - \frac{n_2}{1 - n_2 t} = 0$$

or, or expanding and neglecting terms in t^2 :

$$t = \frac{n_1 + n_2 - n_{12}}{2 n_1 n_2} \quad \text{--- (4)}$$

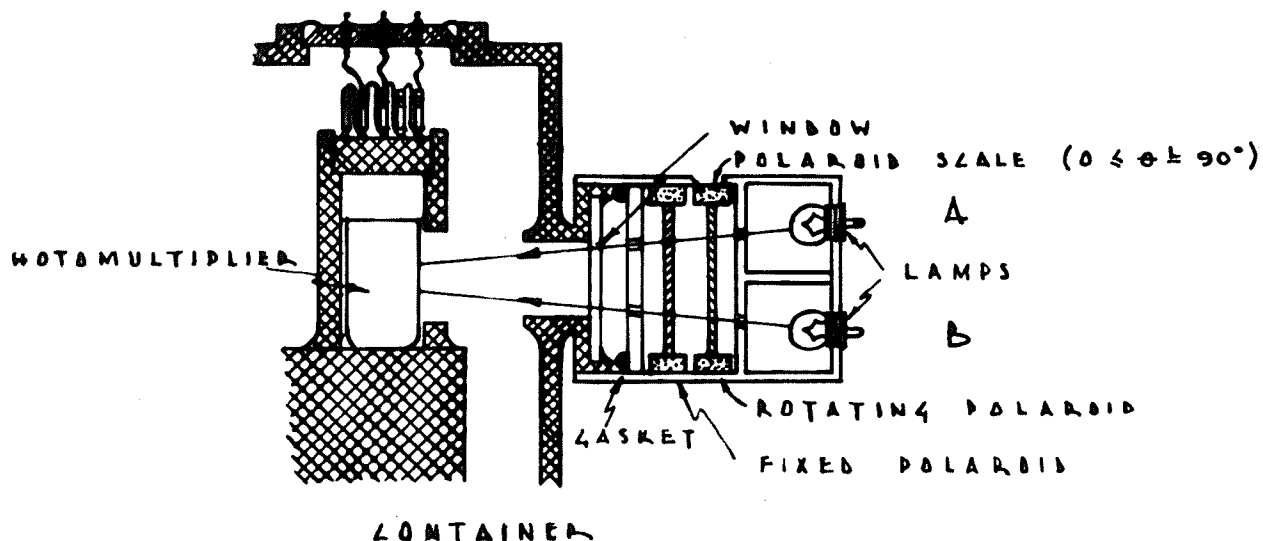


FIGURE 14
 DOUBLE LIGHT SOURCE FOR
 MEASURING CIRCUIT RESOLVING TIME

TABLE 3

$I_A = 175 \text{ M.A.}$

$I_B = 170 \text{ M.A.}$

$\theta = 70^\circ$

TRIAL	n_1 (counts/sec.)	n_2	n_{12}	τ
1	117.2	113.1	229.8	$19.0 \times 10^{-6} \text{ sec.}$
2	113.8	104.7	218.2	$12.5 \times 10^{-6} \text{ sec.}$
3	120.5	117.0	237.1	$14.2 \times 10^{-6} \text{ sec.}$
AVERAGE RESOLVING TIME:				<u>$15. \times 10^{-6} \text{ sec.}$</u>

The above procedure was carried out with the filament currents of lamps "A" and "B" 175 milliamperes and 170 milliamperes respectively and the polaroid axes at 70° . The observed individual and combined counting rates are shown in Table 3, together with the calculated resolving times. The average of the resolving times obtained in four separate trials was about 15 microseconds.

EFFICIENCY OF THE DETECTING SYSTEM

If we assume a photon incident on the cathode of the photomultiplier transfers all its energy to a single electron by a photoelectric collision, then this electron will have a probability of escape, P_1 , dependent on the photon energy and the nature of the emitting surface. If emitted, the electron will then have a certain probability, P_2 , of producing an observable pulse dependent on, among other factors, the average secondary emission ratio and the pulse-height discrimination level. The product $P = P_1 P_2$ gives the probability that a photon incident on the cathode will produce an observable pulse. This probability will be called the "efficiency" of the system. The following

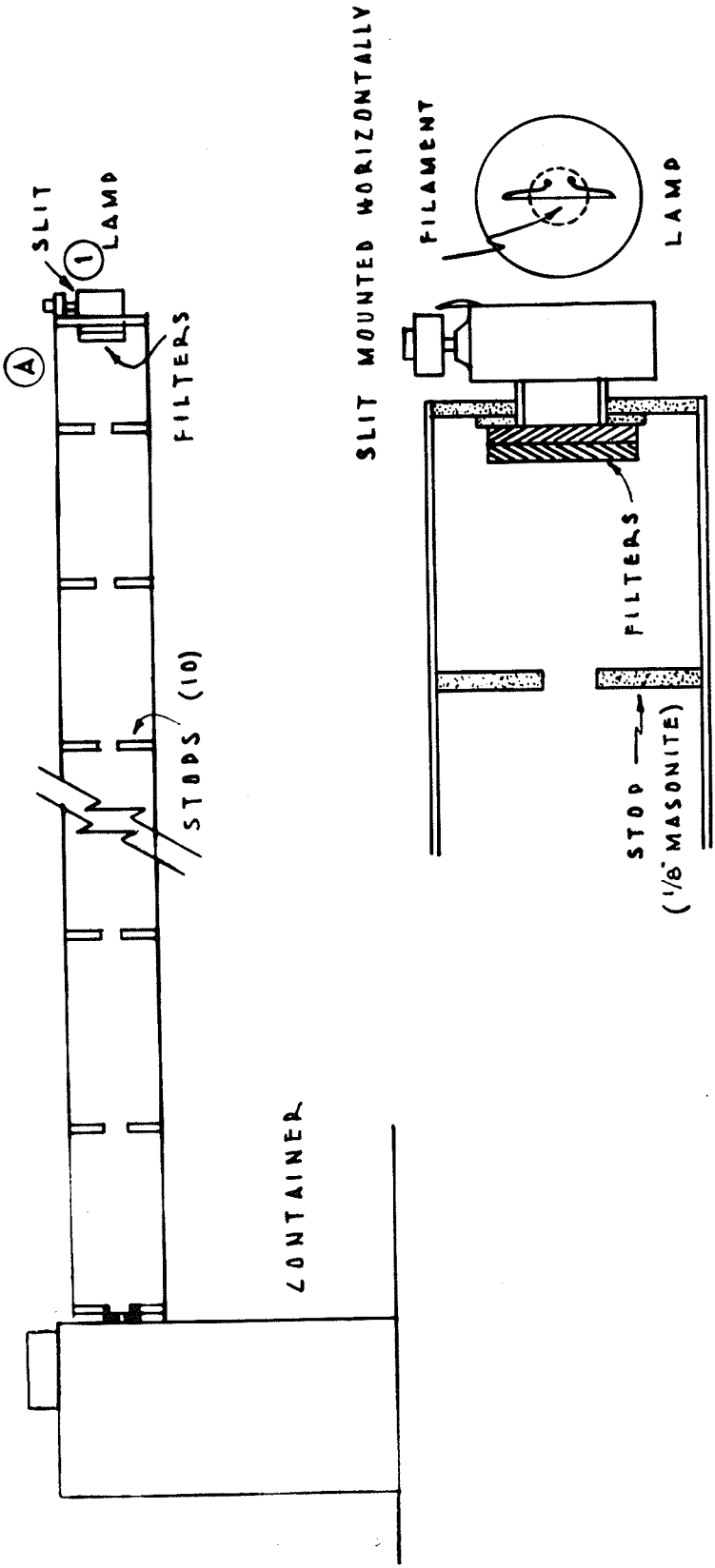
experiment was designed to measure this efficiency at a given wavelength and intensity of illumination.

To facilitate the calculation of the amount of energy reaching the cathode, a galvanometer lamp with a straight tungsten filament was chosen as a source of illumination. This allowed the use of a set of tables of tungsten filament characteristics compiled by Langmuir and Jones⁽⁸⁾, reproduced in part in Table 3.

The lamp, with its filament in a vertical plane, was placed at one end of a cylindrical tube about 13 feet long. The tube, which consisted of a number of four inch stovepipe sections painted a dull black on the inside, was fastened at the other end over the window of the photomultiplier container, (Figure 15). A number of stops, placed at random intervals in the tube, minimized the possibility of any reflected light reaching the photomultiplier. The filament was blacked off vertically by a horizontal spectroscopy slit so that only a small central section was visible to the multiplier. The slit width was determined directly from the calibrated drum reading. A filter combination, consisting of a Baird interference filter (#7-2129A) and a Corning 5031 absorption filter, having a narrow transmission band

TUNGSTEN FILAMENT CHARACTERISTICS

WATTS INPUT $W' = W/d$ (watts/cm ²)	TEMPERATURE T (Absolute degrees)	WATTS RADIATED $\bar{W} = W/\pi d$ (watts/cm ²)	EMISSIVITY (Black body = 1)	$\frac{V \sqrt{I}}{l}$ volts amps ^{1/3} cm ⁻¹
1.891	1000	0.602	0.105	48.42 x 10 ⁻³
3.223	1100	1.027	0.124	71.78
5.210	1200	1.66	0.141	102.3
8.060	1300	2.57	0.158	141.3
12.01	1400	3.83	0.175	189.8
17.33	1500	5.52	0.192	249.0
24.32	1600	7.74	0.207	320.1
33.28	1700	10.62	0.222	404.0
44.54	1800	14.18	0.237	502.0
58.45	1900	18.64	0.250	614.6



DETAIL AT (A)

FIGURE 15
 LIGHT SOURCE FOR
 PHOTOMULTIPLIED CALIBRATION

at 4620 Å, was fastened behind the slit.

Power for the lamp was supplied by six number 6 dry cells in parallel, connected in series with a 100 ohm "Heliopot" rheostat and milliammeter, the voltage drop between the leads being measured with a vacuum tube voltmeter. The filament length was measured with a cathetometer, its diameter with a micrometer, the bulb being broken to make the latter measurement after the experiment was completed. The diameter measurement was extremely inaccurate due to the small filament size and was used only to check the diameter calculated from the functions given in the Table.

Now if the voltage drop across the filament V , is known, as well as the filament current I , and filament length l , the value of the function $\frac{V\sqrt{I}}{l}$ may be calculated. The corresponding value of $W' = \frac{W}{ld}$ (where $W = VI$) may then be found by interpolation on the tables, and the filament diameter d , determined. However, the value of V must be corrected for the voltage drop in the leads. If we let the measured value be V' , then:

$$V = V' - IR'$$

where R' is the lead resistance. Assuming the leads to be at room temperature:

$$R' = \frac{4\rho l'}{\pi(d')^2}$$

where ρ = resistivity of tungsten at 293°K.

$$= 5.49 \text{ microhm cm.}$$

l' = total lead length

d' = lead diameter.

$$\text{Then } V = V' - \frac{4I\rho l'}{(d')^2} \quad \text{----- (1)}$$

The temperature, T , of the filament and its emissivity, E , may be obtained from the tables once the value of $V\sqrt{I}/l$ is known. E is defined as the ratio of the total energy per square centimeter radiated by the filament to that radiated by a black body at the same temperature. The spectral emissivity E_λ , on the other hand, is defined as the ratio of the energy per square centimeter radiated by the filament to that radiated by a black body at the same temperature at a given wavelength λ . Since the colour temperature of tungsten is approximately equal to its actual temperature⁽⁹⁾ E_λ will be more or less constant throughout the spectral region with which we are concerned, and will be approximately equal to E .

Consequently, knowing E , we may use the Planck equation to estimate the amount of energy radiated by one square centimeter of filament surface between the transmission limits of the filter combination. For a black body:

$$W_\lambda = J_\lambda d\lambda = \frac{c, d\lambda}{\lambda^5 \left(e^{\frac{c}{\lambda T}} - 1 \right)} \quad \text{----- (2)}$$

where $W_\lambda =$ watts radiated per square cm.

in a spectral band of width $d\lambda$ at wavelength λ .

$T =$ the temperature of the black body in absolute degrees.

$$C_1 = 3.697 \times 10^{20} \text{ watts angstroms}^4 \text{ cm.}^{-2}$$

$$C_2 = 1.432 \times 10^8 \text{ angstrom degrees. (10)}$$

Then if \bar{W}_λ is the number of watts radiated per square centimeter in the same spectral band by the filament, we may write:

$$\bar{W}_\lambda = \int W_\lambda = \frac{E_c d\lambda}{\lambda^5 (e^{C_2/T} - 1)} \quad \text{--- (3)}$$

Now if the spectroscopy slit, of width l_s , is placed at a distance R from the cathode, and the filament at a distance $R' > R$ then the effective projected filament length is given by:

$$l_f = \frac{l_s R'}{R} \quad \text{--- (4)}$$

Care must be taken in choosing R' and R so that the cathode lies completely within the umbra of the illumination from the filament.

We are concerned then with a section of the filament of length l_f and diameter d . The total energy radiated from this section within the transmission limits of the filter will be given by:

$$N = \bar{W}_\lambda \pi l_f d.$$

To find the energy flux per unit solid angle normal to the filament axis we make two assumptions: 1) the distribution of energy is radially symmetrical about the filament; 2) the distribution in a vertical plane through the filament obeys Lambert's cosine law. Then the energy flux through the surface of a vertical segment $d\phi$ (Figure 16) will be given by $N \frac{d\phi}{2\pi}$. If we let τ be the flux per unit solid angle normal to the filament, then the flux at an angle θ to the normal will be given by $\tau \cos \theta$. In particular the energy passing through the element of surface $dA = p^2 \cos \theta d\theta d\phi$, will be given by:

$$\frac{\tau \cos \theta dA}{p^2} = \tau \cos^2 \theta d\theta d\phi$$

$$\text{Then: } \int_{\theta = -\pi}^{\pi} \tau \cos^2 \theta d\theta d\phi = N \frac{d\phi}{2\pi}$$

$$\text{and } \tau = \frac{N}{2\pi \int_{-\pi}^{\pi} \cos^2 \theta d\theta} = \frac{N}{2\pi^2}$$

$$\text{But: } N = \overline{W}_\lambda \pi l_f d$$

$$\therefore \tau = \frac{\overline{W}_\lambda l_f d}{2\pi} \quad \text{----- (5)}$$

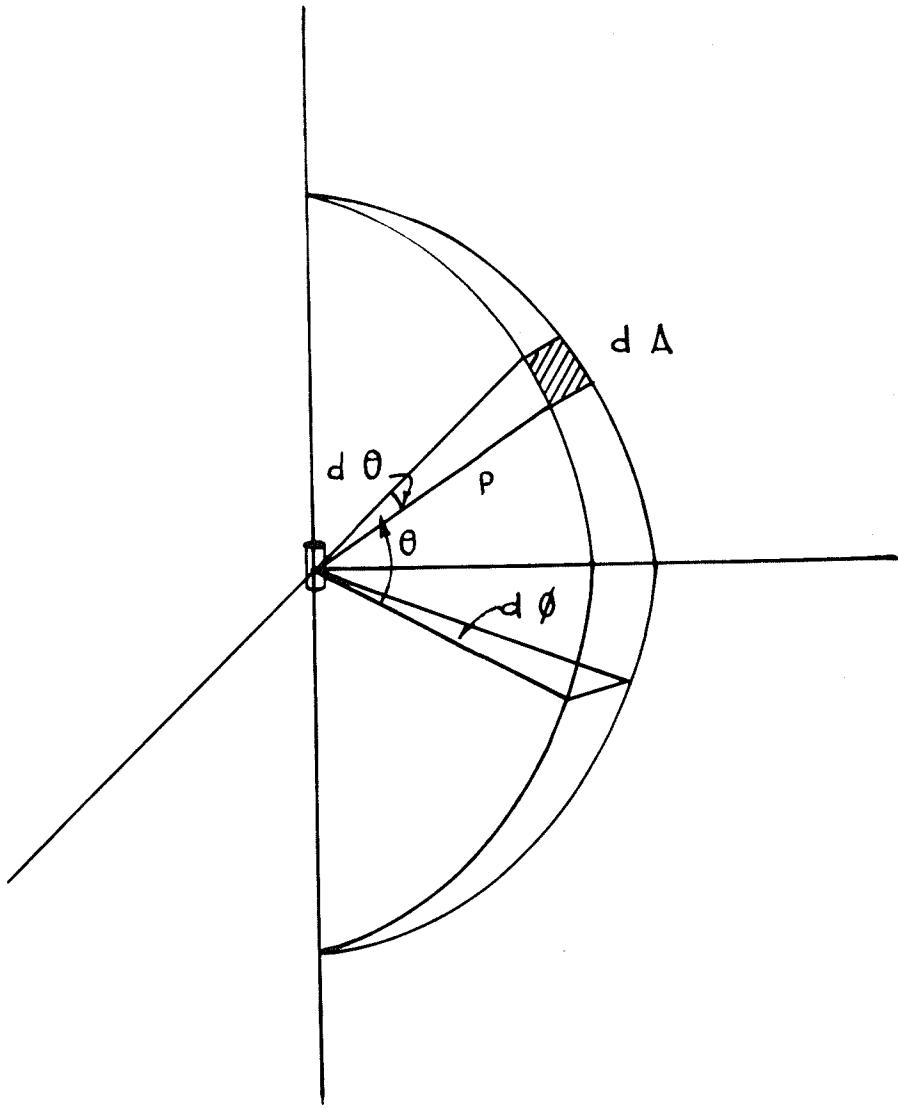


FIGURE 16

If the filter passes $n\%$ of the energy in the transmission band, then the total energy per unit solid angle arriving at the cathode, will be:

$$\tau' = \frac{n\tau}{100} = \frac{n}{100} \frac{E_{c, d\lambda}}{\lambda^5 (e^{\frac{c}{\lambda T}} - 1)} \cdot \frac{l_f d}{2\pi} \text{ ----- (6)}$$

The solid angle subtended at the filament section by the cathode is given by: $S/(R')^2$ where S is the projected cathode area normal to the line joining the filament and cathode. The total amount of energy reaching the cathode, then, is given by:

$$\bar{E} = \frac{S \tau'}{(R')^2} \text{ ----- (7)}$$

Using the units indicated \bar{E} will be in watts. The energy in ergs per second will be given by $\bar{E} \times 10^7$. Now each photon of wavelength λ has an energy is given by:

$$E_p = h\nu = \frac{hc}{\lambda \times 10^{-8}} \text{ ----- (8)}$$

where E_p = photon energy in ergs

c = velocity of light = 2.998×10^{10} cm./sec.

λ = wavelength in angstroms.

h = Planck's constant

= 6.6608×10^{-27} erg-sec.

The number of photons per second falling on the cathode will be given then by:

$$N = \frac{E \times 10^7}{E_p} = \frac{10^7 S}{(R')^2} \cdot \frac{\pi}{100} \cdot \frac{E c_1 d \lambda}{\lambda^5 (e^{\frac{c_2}{\lambda T}} - 1)} \cdot \frac{l_f d}{2\pi} \cdot \frac{\lambda \times 10^{-8}}{hc}$$

$$\text{i.e. } N = \frac{S \pi l_f d}{2\pi (R')^2} \cdot \frac{E c_1 d \lambda \times 10^{-3}}{hc \lambda^5 (e^{\frac{c_2}{\lambda T}} - 1)} \text{ ----- (9)}$$

Experimental Results

a) Voltage drop across filament leads,

$$V' = 0.75 \pm 0.01 \text{ volts}$$

Filament current,

$$I = 200 \pm 2 \text{ milliamperes}$$

Filament length,

$$l = 1.795 \pm 0.005 \text{ cm.}$$

Filament leads,

$$\text{Total length } l' = 5.00 \pm 0.05 \text{ cm.}$$

$$\text{diameter } d' = (28.0 \pm 0.5) \times 10^{-3} \text{ cm.}$$

(1) From equation (1):

$$V = 0.75 = \frac{4(200 \times 10^{-3})(5.49 \times 10^{-6})(5.00)}{(28)^2 \times 10^{-6}}$$

$$= 0.74 \text{ volts.}$$

$$(2) \frac{V \sqrt[3]{I}}{l} = \frac{0.74 \sqrt[3]{200} \times 10^{-1}}{1.795} = 0.241 \text{ volt amperes}^{1/3} \text{ cm.}^{-1}$$

Then by interpolation on the tables:

$$W' = \frac{W}{ld} = 16.7 \text{ watts/cm.}^2$$

$$d = \frac{W}{W'l} = \frac{0.74 \times 200 \times 10^{-3}}{16.7 \times 1.795} = 4.93 \times 10^{-3} \text{ cm.}$$

Measured value of d: $(5.0 \pm 0.5) \times 10^{-3}$ cm.

b) Slit width $l_s = 0.705 \pm .005$ mm.

$$R = 430 \pm 3 \text{ cm.}$$

$$R' - R = 5.7 \pm 0.1 \text{ cm.}$$

$$R' = 435.7 \text{ cm.}$$

From equation (4):

$$l_f = \frac{435.7}{430} \times 0.0705 = 7.14 \times 10^{-2} \text{ cm.}$$

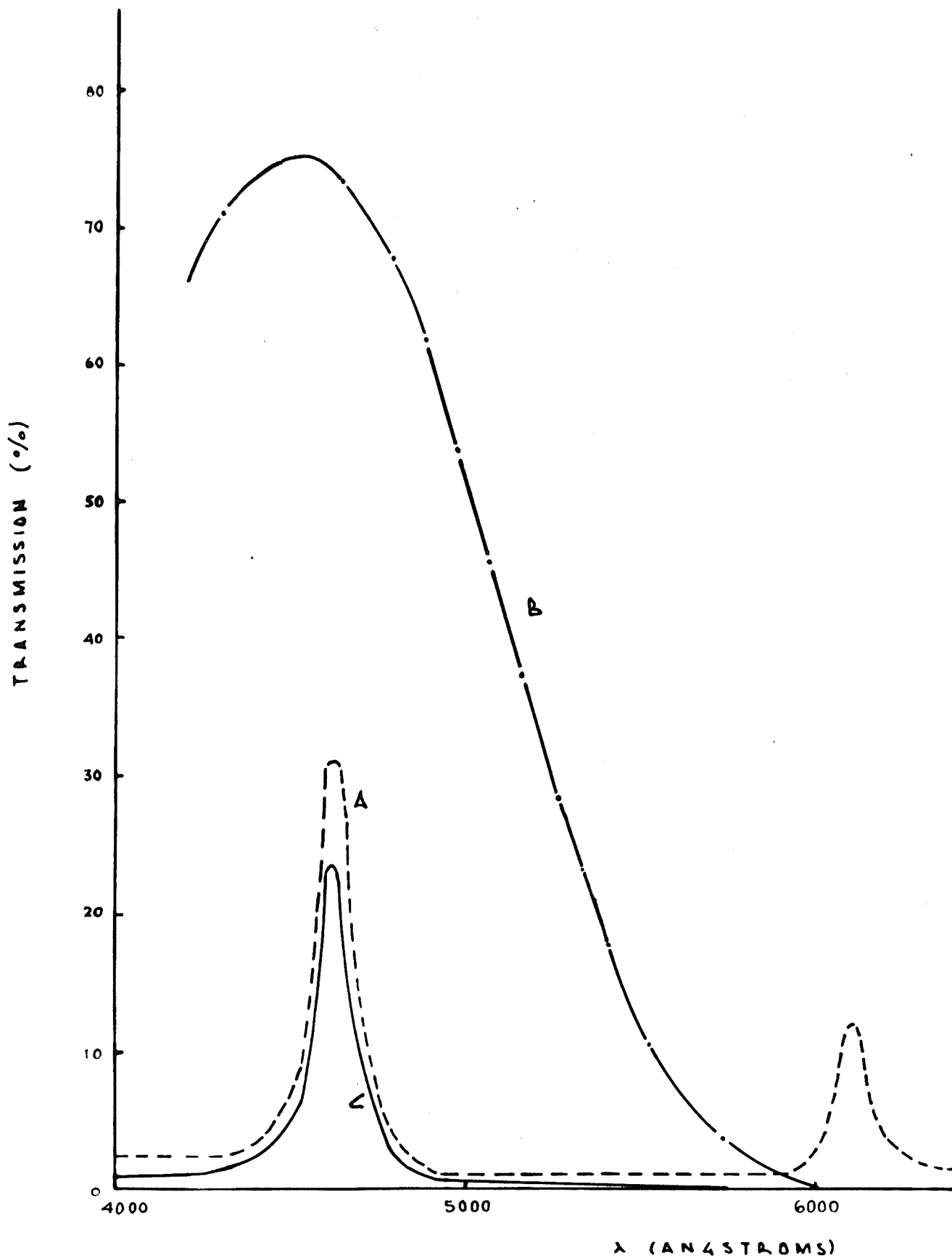
c) From interpolation on the tables $T = 1490^\circ\text{K.}$

d) The absorption curves for the filters, supplied by the respective manufacturers, are given in Figure 17. The combined filters have a transmission band at 4620 Å with an average width of 150 Å and 23.5% transmission.

$$n = 23.5$$

$$\lambda = 4620$$

$$d = 150$$



- - - - - BAIRD 7-2129 A
 ——— LORNING 5031
 ——— COMBINATION

FIGURE 17
 FILTER TRANSMISSION BANDS

e) The projected cathode area,

$$s = 2.54 \times 0.95 = 2.42 \text{ cm}^2$$

f) Using these values in equation (9) yields:

$$N = \frac{(2.42)(23.5)(7.14 \times 10^{-2})(4.93 \times 10^{-3})}{2\pi(435.7)^2} \times \frac{(.190)(3.697 \times 10^{-20})}{(6.66 \times 10^{-27})(2.998 \times 10^{10})}$$

$$\times (150 \times 10^{-3})$$

$$\frac{(4620)^4 \left[\frac{1.432 \times 10^8}{(4620)(1490)} - 1 \right]}{e}$$

$$= 1.70 \times 10^3 \text{ photons/second.}$$

$$= 1.02 \times 10^5 \text{ photons/minute.}$$

g) Counts above background recorded at 100 volts/stage and 1.0 M.V. discrimination level:

$$745 \text{ counts/minute.}$$

h) The efficiency of the detecting system:

$$P = \frac{7.45 \times 10^2}{1.02 \times 10^5} \approx 7.3 \times 10^{-3}$$

That is to say, at the given wavelength and intensity of illumination there is, on the average, one observable pulse for approximately every 140 photons arriving at the cathode.

Corrections

The accuracy of the foregoing calculations depends largely on the applicability of the tables to the filament used. The tables were compiled for "ideal" tungsten filaments; that is, filaments in a good vacuum, of well-aged tungsten, and with no heat loss due to the leads. The lamp manufacturers (General Electric Co.) supplied the information that the filament was of pure tungsten in a vacuum, and the authors (Langmuir and Jones) state that the normal vacuum found in commercial lamps is sufficient to have a negligible effect on the heat lost by the filament. The largest error then, will lie in the heat conducted away from the filament by the leads, resulting in a lower filament temperature than that estimated, and consequently a reduction in the amount of energy radiated. This effect was kept to a minimum by using only a small centre section of the filament. The temperature here will be a maximum and could reasonably be expected to be close to that given in the tables.

There is, however, a correction to be made for absorption and reflection by the bulb. The absorption in a clear glass bulb, according to Langmuir and Jones, is about 1%, and total reflection, considering both surfaces, about 8.3%. Reflected and refracted light entering the slit indirectly from the bulb itself was kept at a minimum by blocking off the slit laterally with black tape to a width of about two millimeters.

Reflection and absorption at the window of the photomultiplier container is ignored, as this is considered an integral part of the system.

The energy radiated, then, should be reduced by about 9%, increasing the efficiency slightly. This, of course, is at best a good approximation. A slight contamination of the tungsten alone could introduce considerable error. A more accurate determination could have been made by having the lamp and filters calibrated by the National Bureau of Standards before performing the experiment.

SPECTRAL RESPONSE OF THE SYSTEM

In order that the illumination studied may be properly analyzed, the spectral response of the system must be determined. This was done by setting up the lamp mentioned in the previous experiment at an appropriate distance from the input slit of the monochromator and measuring the resultant activity at a number of wavelength settings. The multiplier was operated at 100 volts per stage with a one millivolt discrimination level.

Experimental Results

- a) The spectral response to the light source used is shown in Figure 18(A).

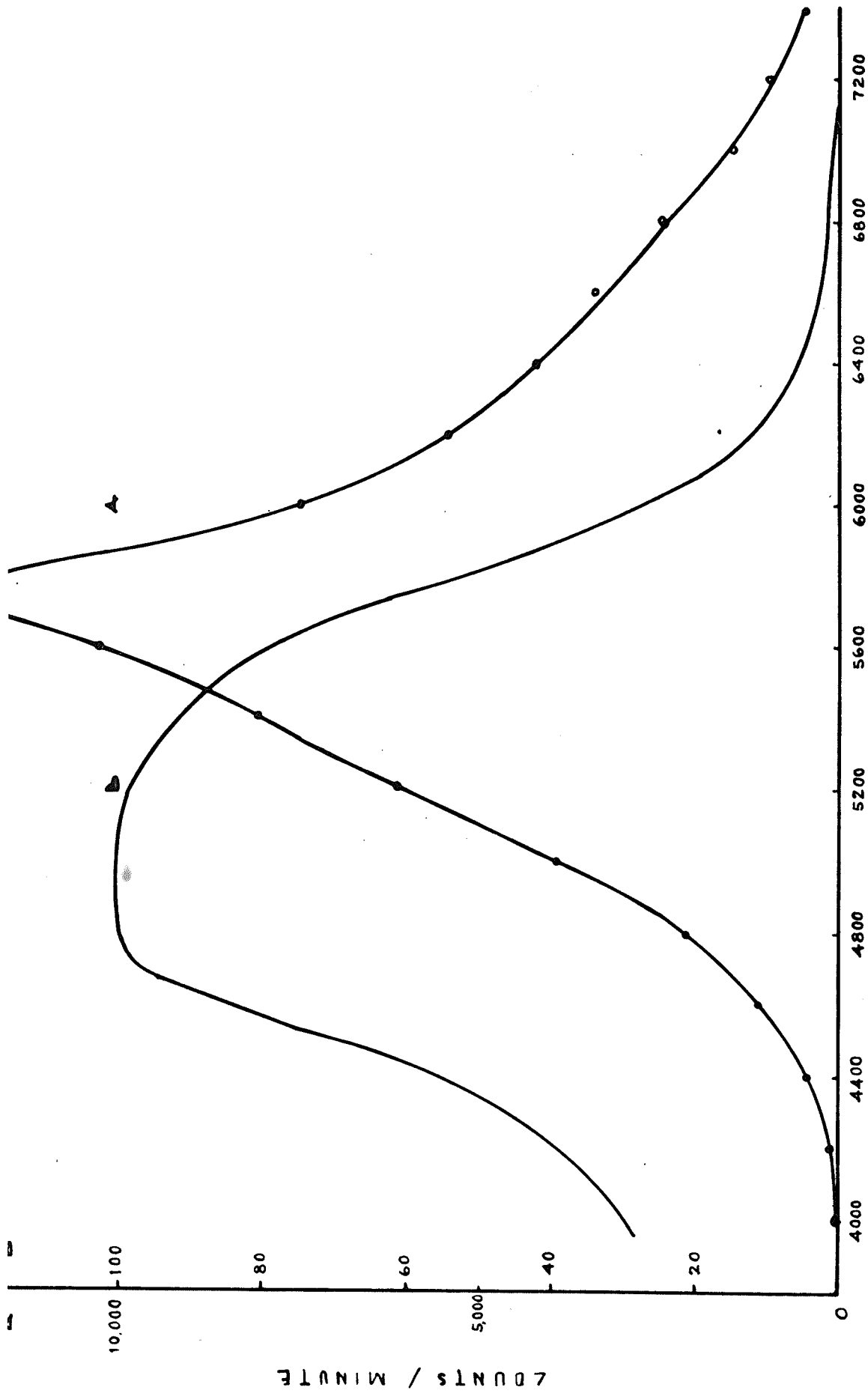


FIGURE 18

A—SPECTRAL RESPONSE OF 931A TUBE LAMP WITH $T_e = 1870^\circ K$.

B—RELATIVE RESPONSE TO A SOURCE WITH UNIFORM PHOTON DENSITY

b) Voltage between filament leads: $V' = 1.59 \pm 0.01$ V.

filament current $I = (300 \pm 2) \times 10^{-3}$ A.

Using equation (1) of the previous section:

$$V = \frac{V' - 4 I \rho' l'}{(d')^2}$$

$$= 1.58 \text{ v.}$$

$$\text{Then } \bar{W} = \frac{W}{\pi l d} = \frac{VI}{\pi l d} = \frac{(1.58)(300) \times 10^{-3}}{(1.795)(4.93) \times 10^{-3}} = 17.08 \text{ watts/cm}^2$$

Then by interpolation on table 3:

$$T = 1870^\circ \text{ K.}$$

The spectral distribution of radiation from a black body at this temperature may be obtained from the Planck equation:

$$W_\lambda = J_\lambda d\lambda = \frac{c_1 d\lambda}{\lambda^5 (e^{\frac{c_2}{\lambda T}} - 1)} \quad \text{----- (1)}$$

where $W_\lambda = \text{watts/cm}^2/\text{unit solid angle/angstrom.}$

$\lambda = \text{wavelength in angstroms.}$

$d\lambda = \text{wavelength interval in angstroms.}$

$T = \text{absolute temperature of the body.}$

$c_1 = 1.177 \times 10^{20} \text{ watts angstroms}^4 \text{ cm.}^{-2} \text{ steradian}^{-1}$

$c_2 = 1.432 \times 10^8 \text{ angstrom degrees.}$

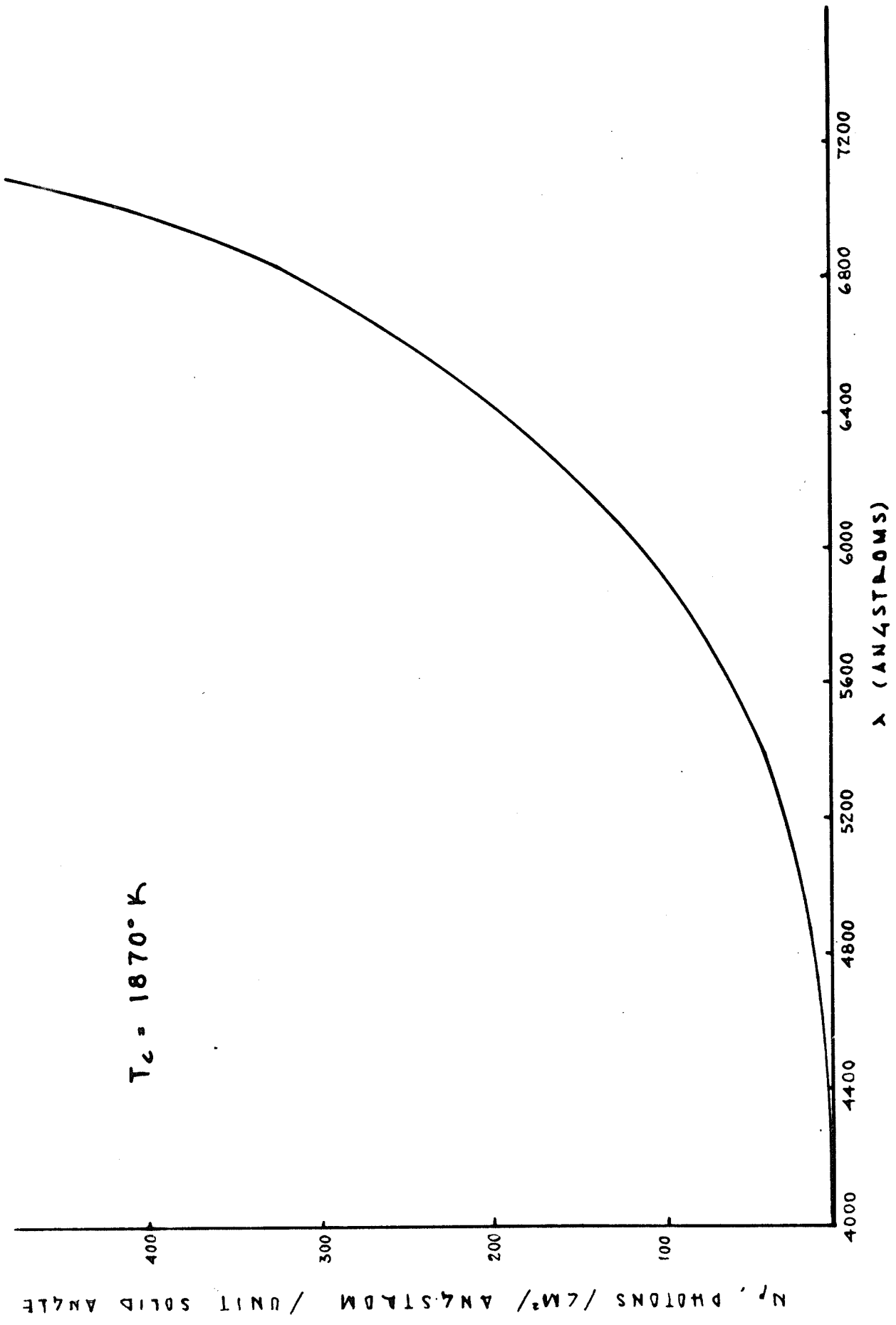


FIGURE 19
DISTRIBUTION OF BLACK BODY RADIATION

This gives the amount of energy in the interval $d\lambda$ at wavelength λ radiated in a unit solid angle from one square cm. of black body at temperature T . We may find the number of photons radiated by dividing by the photon energy at this wavelength:

$$\text{i.e. } N_p = \frac{E_\lambda \times 10^7}{E_p}$$

$$\text{where } E_p \text{ in ergs: } = \frac{hc}{\lambda \times 10^{-8}} \quad (\lambda \text{ in Angstroms})$$

$$\therefore N_p = \frac{c_1 d\lambda}{10\lambda^4 hc \left(e^{\frac{c_2}{\lambda T}} - 1 \right)} \quad \text{----- (2)}$$

The graph of Figure 19 was obtained by computing N_p in one Angstrom intervals ($d\lambda = 1$) 400 angstroms apart, between 4000 and 6400 angstroms.

Now if the ordinates of Figure 18(A) are divided by the corresponding ordinates of Figure 19, then the result will be the relative spectral response of the system, in arbitrary units, to a source having a uniform photon density throughout the spectral range considered. This process was carried out, and the resultant curve plotted in Figure 18(B).

An appropriate multiplication factor was used throughout so that the maximum response could be plotted for convenience as 100.

Engstrom has published spectral response curves for the 931A which have a maximum at about 3700 A.⁽⁸⁾ The rapid decline of response below 4700 A in Figure 18(A) is probably due, then, to absorption in the monochromator and the window of the container.

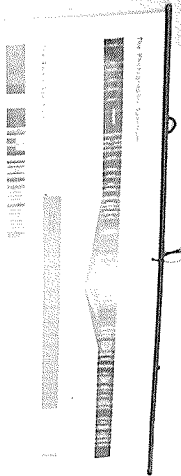
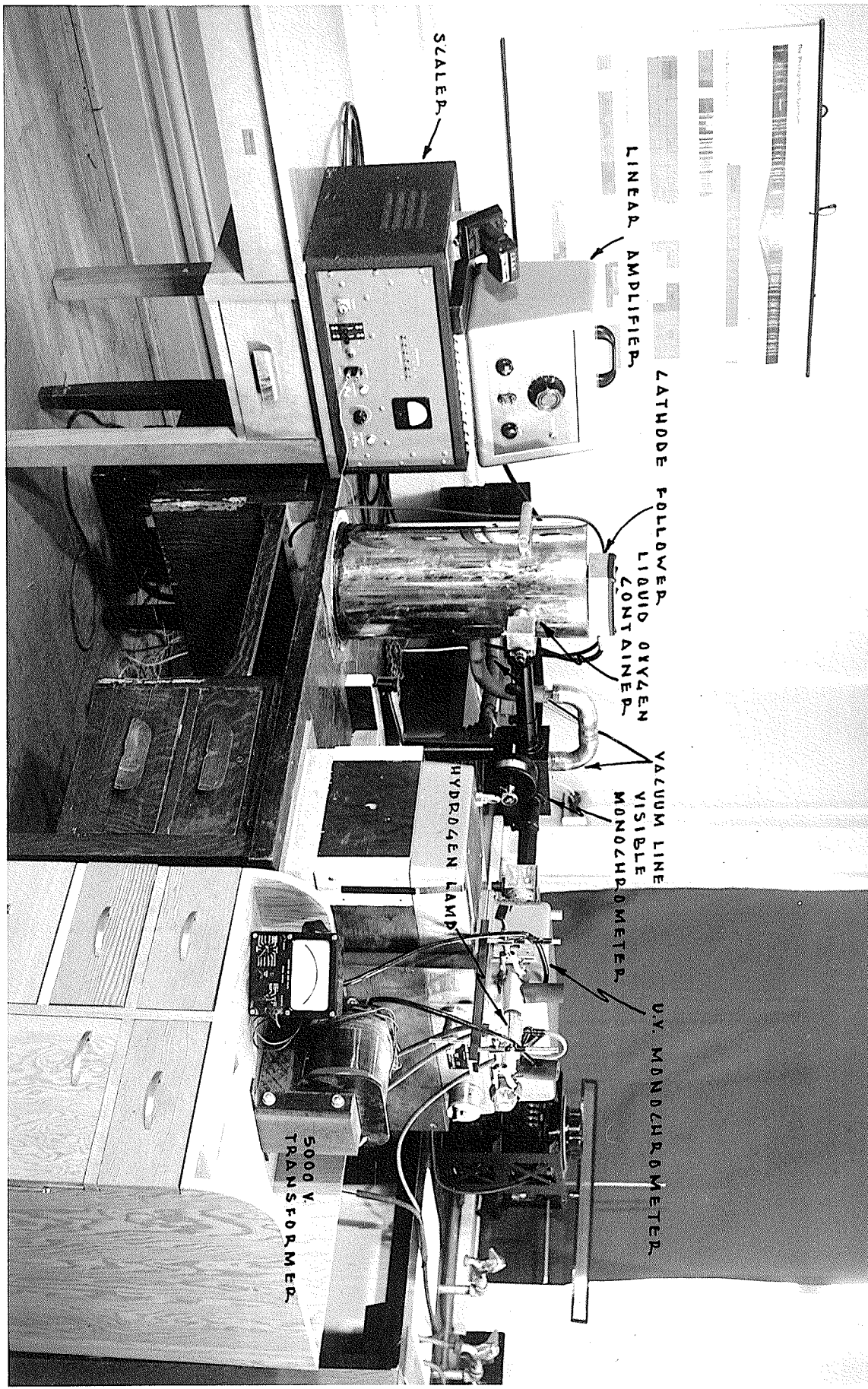
APPLICATION TO THE
ANALYSIS OF FLUORESCENT SPECTRA

The apparatus was used to examine the fluorescence, under ultra-violet radiation, of a number of estrogens in concentrated sulphuric acid, as well as that of urine and blood samples. The exciting radiation from a 5000 volt water-cooled hydrogen tube was passed through a Perkin-Elmer ultra-violet monochromator before being focussed on the solution. This means of irradiation was chosen for two reasons: 1) scattering of the visible portion of the hydrogen spectrum into the detecting unit, and consequent masking of the fluorescence, was prevented; 2) the location of the fluorescent bands is dependent on, among other factors, the wavelength of the excitation, so that in studying the fluorescence, this wavelength is of some interest to the chemist.

The Perkin-Elmer monochromator was a constant-deviation type employing a fixed sixty degree quartz prism, the spectrum being swept across the output slit by means of a rotating front-surfaced mirror. The revolving drum driving this mirror, being graduated in arbitrary units, required calibration. This was done by placing a mercury arc in front of the input slit and a 1P28 photomultiplier with a galvanometer in the anode circuit at the output slit. The drum was then rotated slowly, the presence of a mercury line being indicated by a sudden deflection of the galvanometer. Two of the lines so detected were then positively identified by reflecting the light from the output slit of the Perkin-Elmer

monochromator into the Bausch and Lomb instrument, and adjusting the calibrated wavelength drum of the latter till a maximum activity was produced in the counting system. The lines identified in this manner were at 5461 A and 5791 A. Starting from these points the calibration curve of Figure 20 was drawn using the table of Mercury lines given in the "Handbook of Physics and Chemistry" (Chemical Rubber Publishing Company, 1947).

The two monochromators were then connected by a light-tight brass box with a test-tube holder threaded into the bottom directly below the input slit of the visible instrument. A small test tube in the holder was filled to the top with the solution to be examined and its height adjusted so that the surface of the solution was level with the bottom of the box. The beam emerging from the output slit of the ultra-violet monochromator was reflected by a front surfaced mirror so that it travelled downward at a 45° angle onto the surface of the solution, in a direction perpendicular to the axis of the Bausch and Lomb collimator. This produced a fluorescent spot in the solution about five millimeters in diameter. Some of the fluorescence from this spot was collected by a double concave mirror placed directly over the solution, and reflected horizontally into the collimator slit through a convex lens. The mirror and lens combination was such that the spot image formed at the slit consisted of a thin vertical line about three quarters the slit length.



LINEAR AMPLIFIER

CATHODE FOLLOWER
LIQUID OXYGEN
CONTAINER

VACUUM LINE
VISIBLE
MONOCHROMOMETER

U.V. MONOCHROMOMETER

SCALER

HYDROGEN LAMP

5000 V
TRANSFORMER

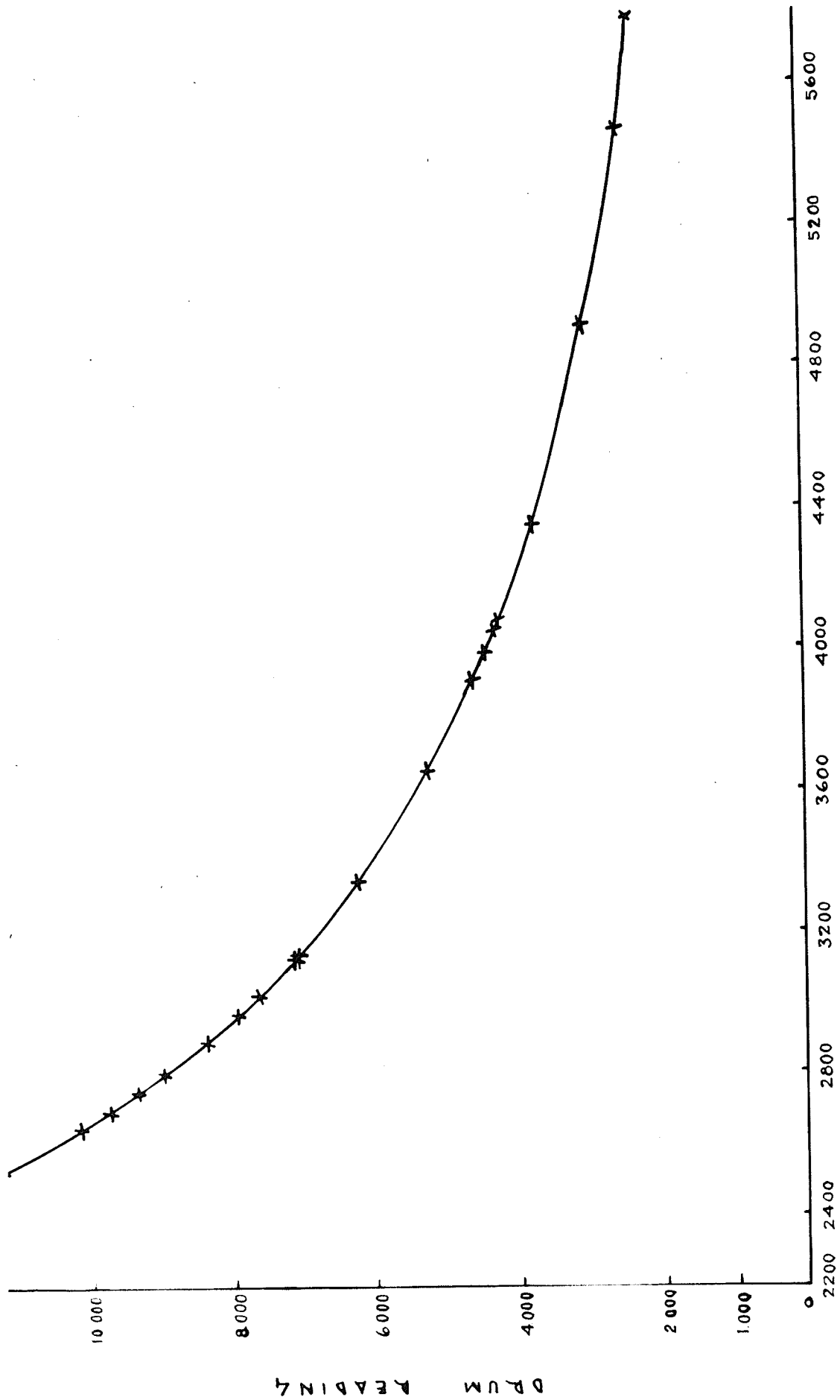


FIGURE 20
CALIBRATION OF

PERKIN - ELMER U.V. MONOCHROMATOR

The photomultiplier was operated at 100 volts per stage with a one millivolt discrimination level, yielding a background of about 45 pulses per minute. The wavelength of the exciting radiation was varied in each case until a maximum activity was obtained and the slits of the Bausch and Lomb instrument closed down as much as possible to obtain maximum resolution. However, some of the fluorescence was extremely weak, requiring the slits to be opened to 0.5 millimeters in order to obtain any appreciable activity. The fluorescent spectra obtained in this manner are illustrated in Figures 21 to 26. These curves were corrected for the response of the 931A by dividing the ordinates by $n/100$ where n is the % response of the multiplier at the wavelength considered, as given in Figure 18(B).

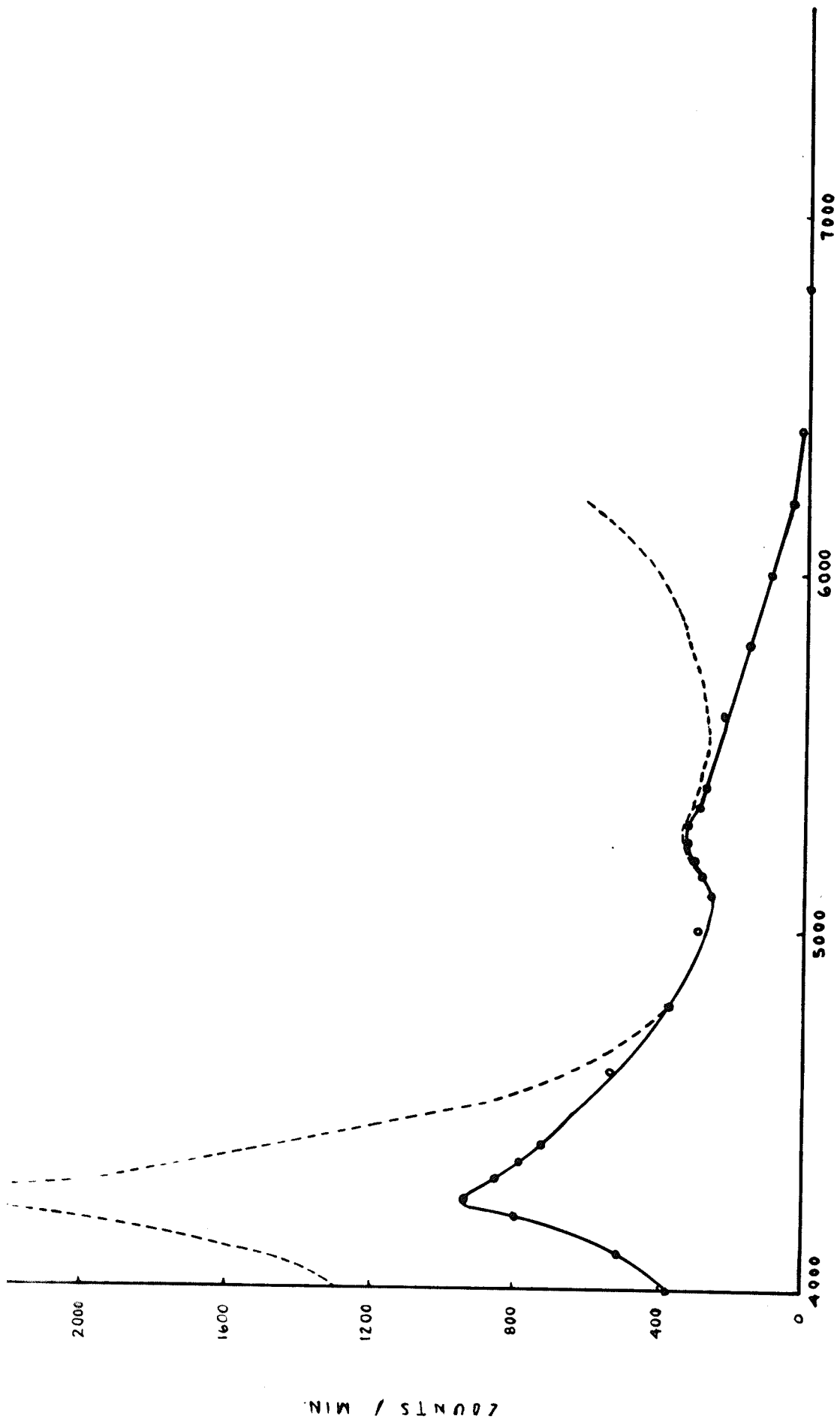
1) 7-Methoxybisdehydrodoisynolic acid

Excited by an ultra-violet band at 3600 angstroms, 52.5 γ (micrograms) of this compound dissolved in 2 ml. concentrated sulphuric acid displayed a strong peak at 4620 A with a weaker one at 5280 A.

2) Ethinyl Estradiol

37 γ in 2 ml. concentrated sulphuric acid, excited by a band at 3600 A, fluoresced weakly with peaks at 4200, 5000 and 5780 angstroms.

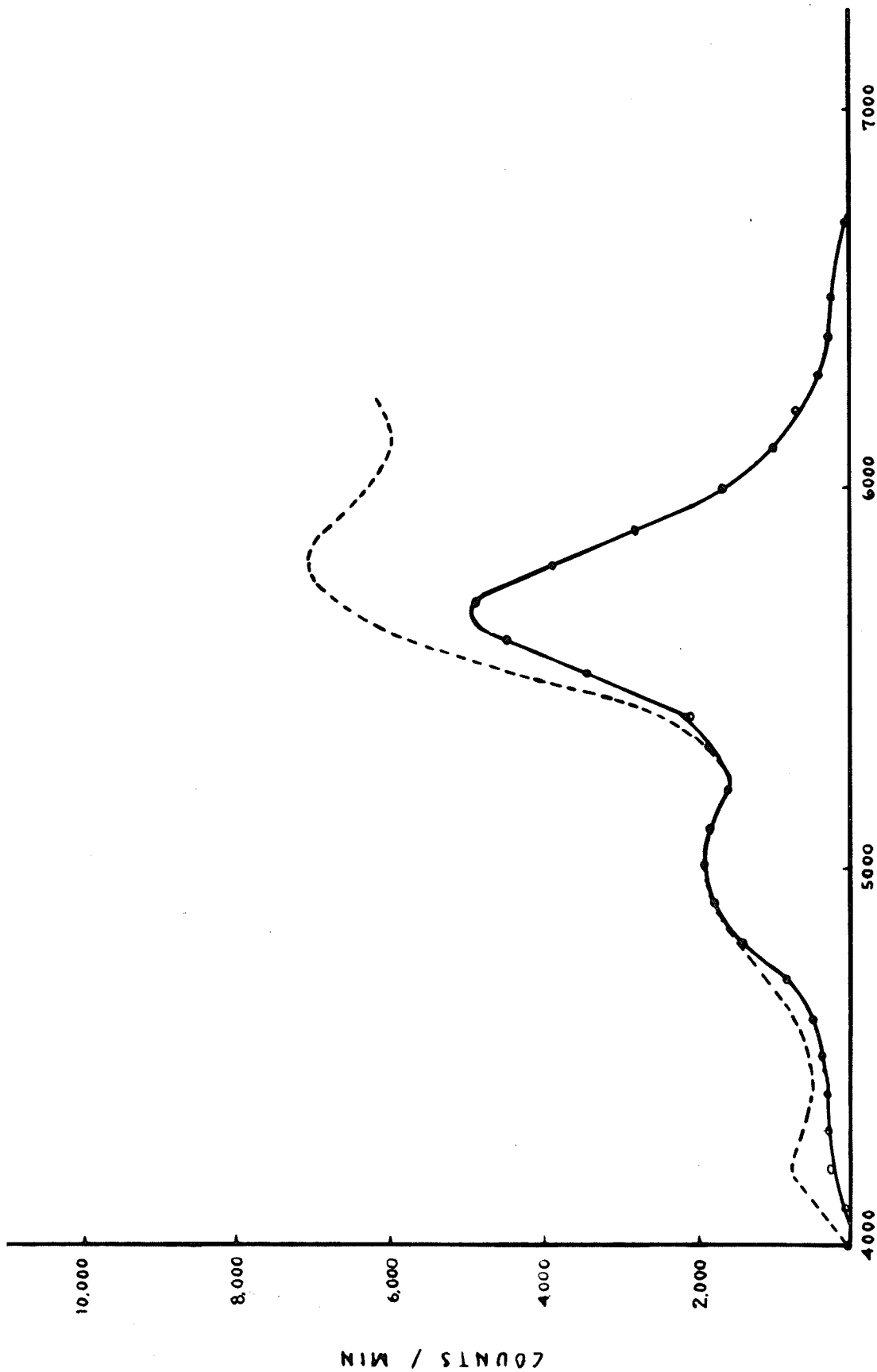




EXCITING LINE 3600 Å
 SLIT WIDTHS 0.05 MM.
 DISC. LEVEL 1.0 M.V.
 VOLTS / STAGE 100
 ----- CURVE CORRECTED FOR 931 Å SPECTRAL RESPONSE IN 2 ML. H₂SO₄

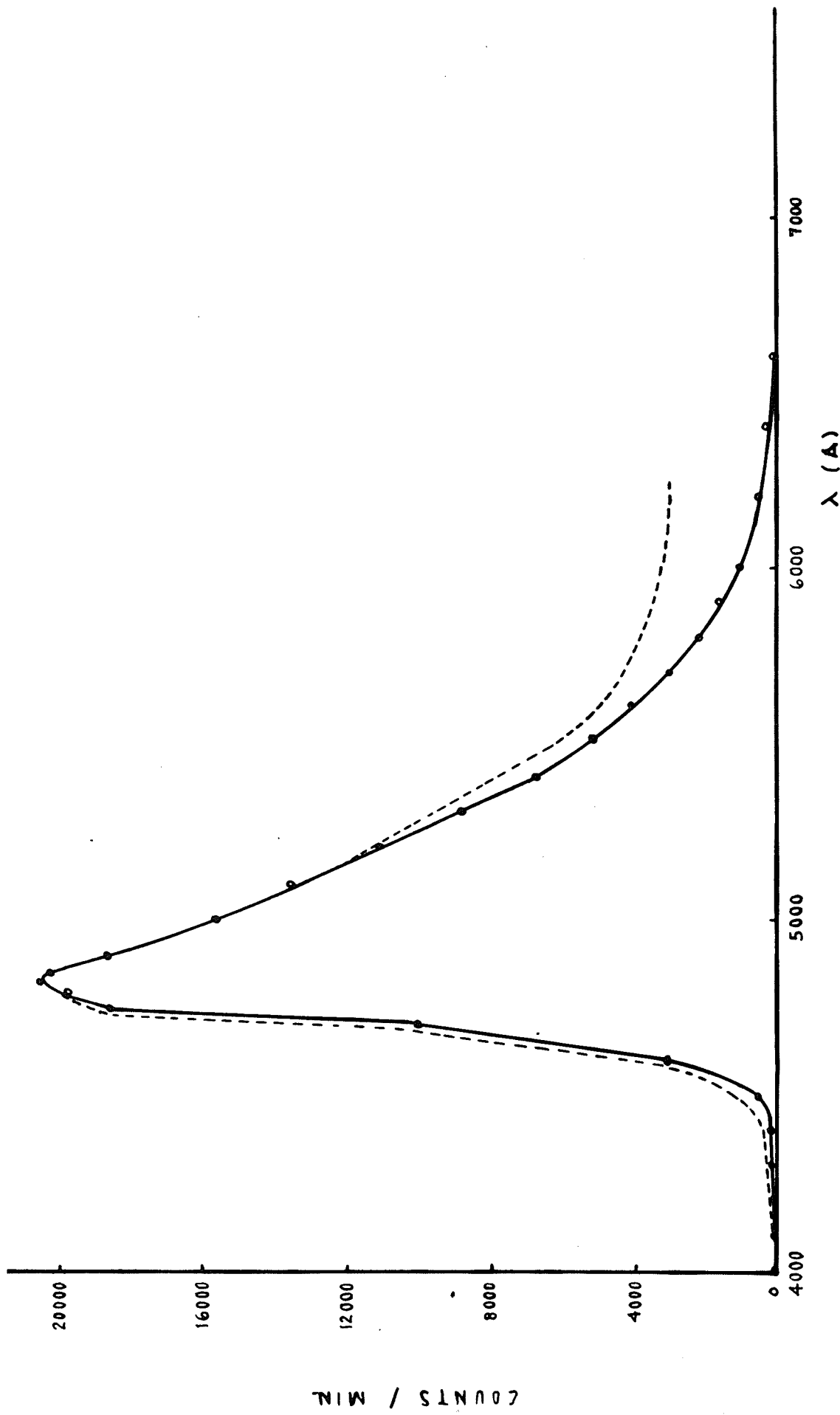
FIGURE 21
 FLUORESCENT SPECTRUM OF
 52.5% 7-METHOXYBISDEHYDRODISYNDILIC ACID

COUNTS / MIN.



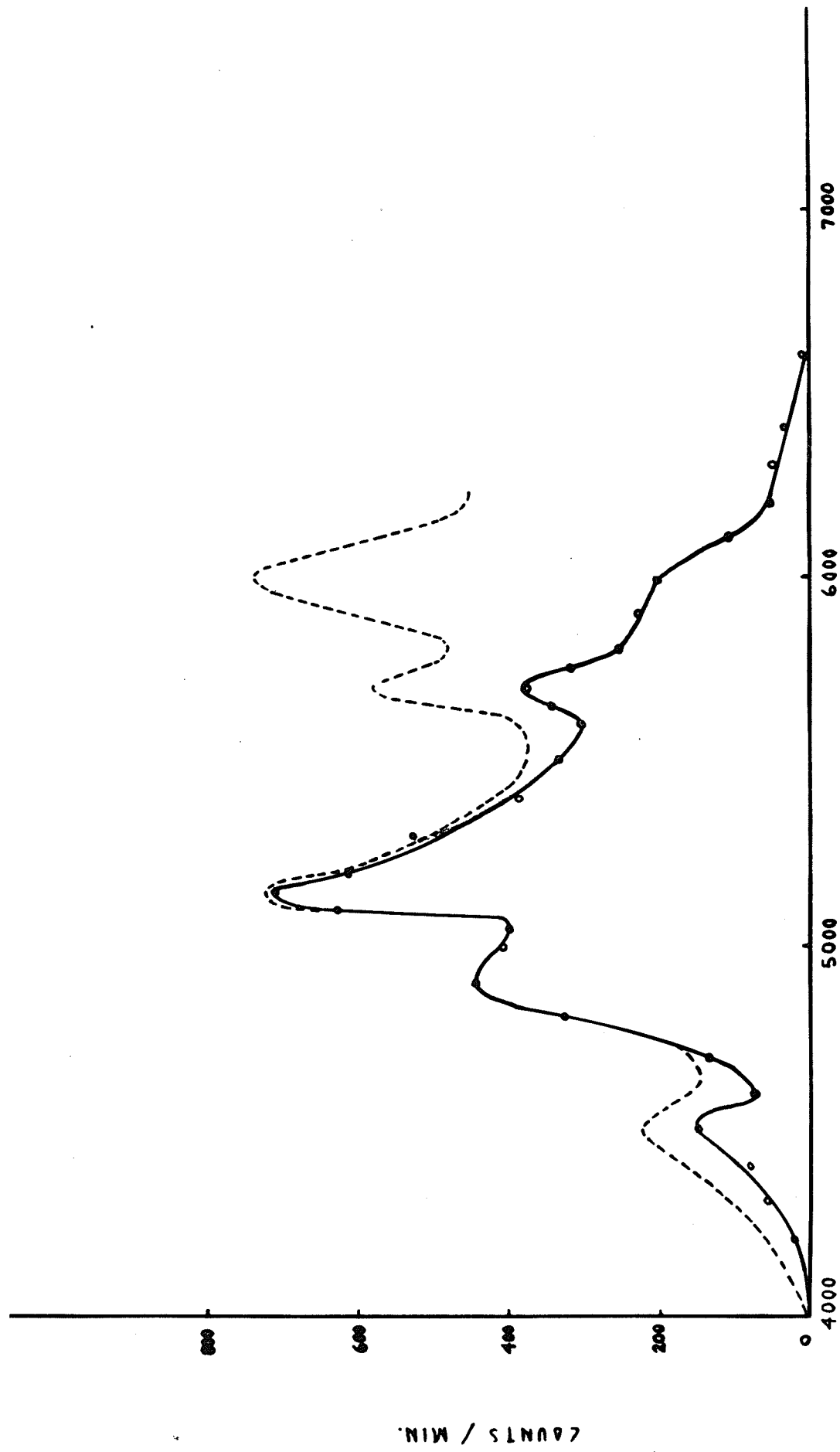
EXCITING LINE 3600 Å
 SLIT WIDTH 0.5 MM.
 VOLTS / STAGE 100
 DISL. LEVEL 1.0 MV.
 ----- CORRECTED

FIGURE 22
 FLUORESCENT SPECTRUM OF
 378 ETHINYL ESTRADIOL
 2 ML. H₂SO₄



EXCITING LINE 3650 Å
 SLIT WIDTH 0.02 MM.
 VOLTS / STAGE 100
 DISC. LEVEL 1.0 MV.
 ----- CORRECTED

FIGURE 23
 FLUORESCENT SPECTRUM OF
 99% ESTRONE IN H₂SO₄



λ (Å)

FIGURE 24

FLUORESCENT SPECTRUM OF

37.5 μ DIENESTROL IN 2 ML. H_2SO_4

EXCITING LINE 3650 Å
 SLIT WIDTHS 0.5 MM.
 DISC. LEVEL 1 M.V.
 VOLTS / STAGE 100
 ----- CORRECTED

COUNTS / MIN.

70007 / MIN.

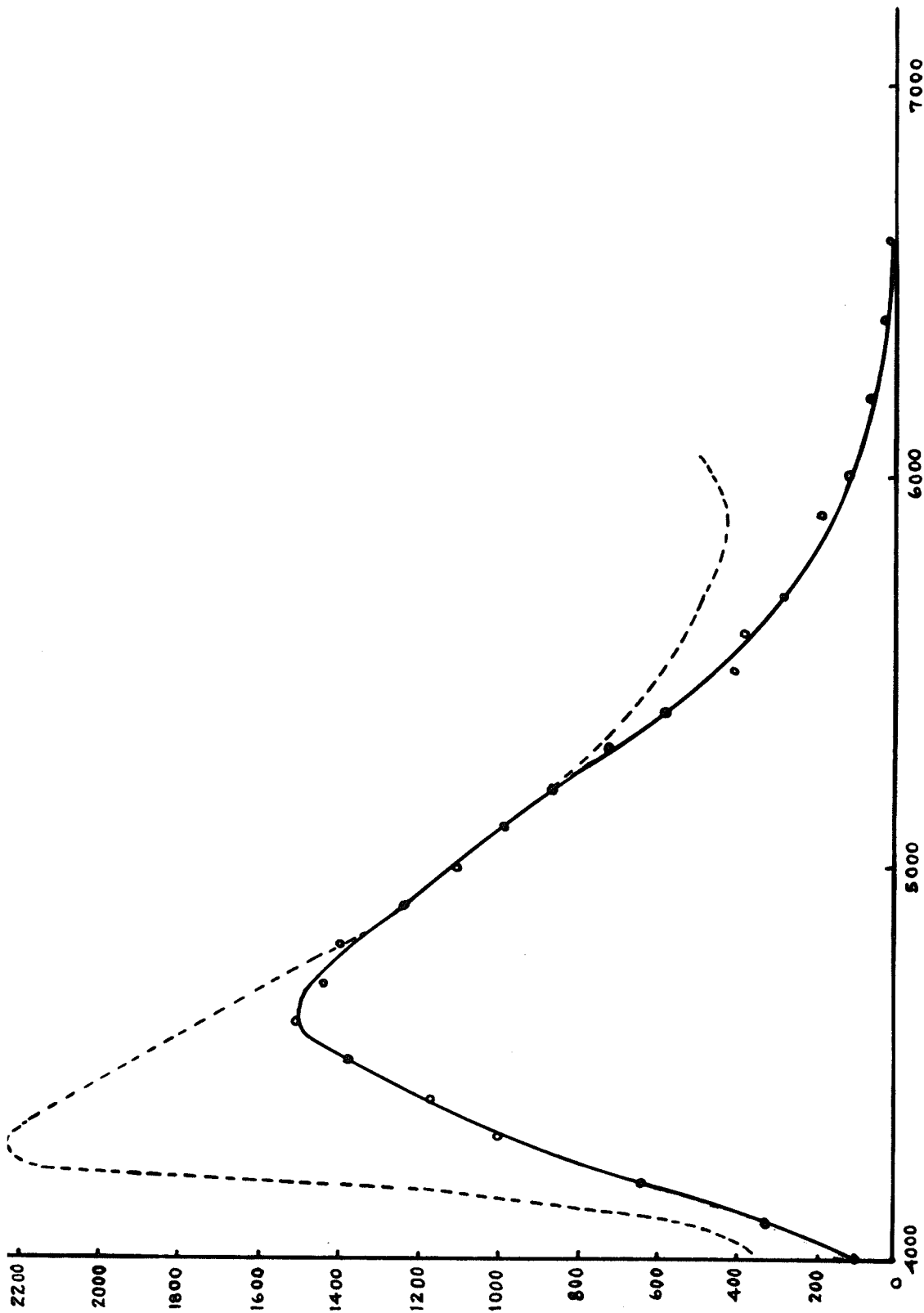
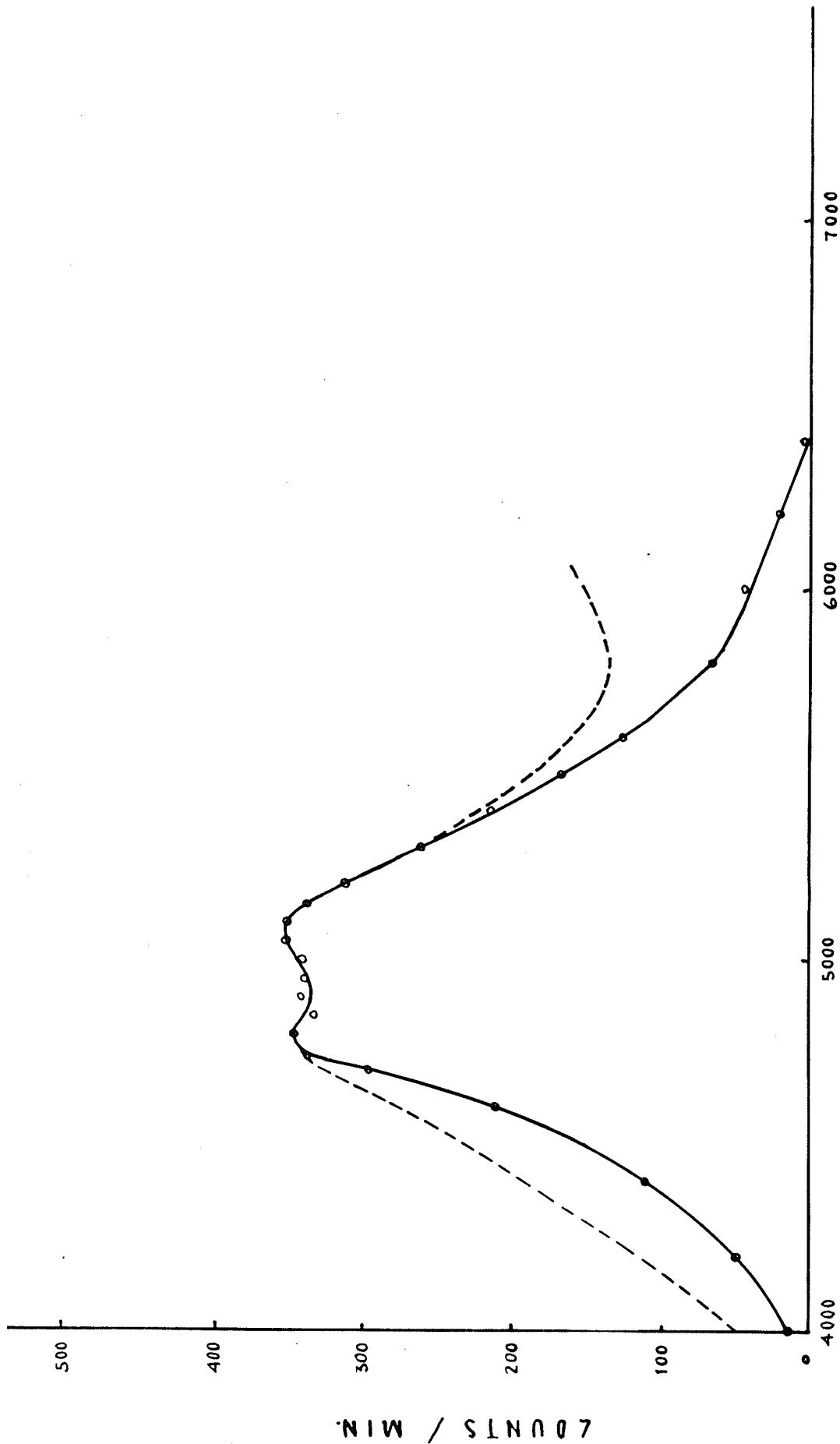


FIGURE 25
FLUORESCENT SPECTRUM OF
MALE URINE SAMPLE

EXCITING LINE 3600 Å
SLIT WIDTH 0.05 MM.
VOLTS / STAGE 100
DISC. LEVEL 10 M.V.
----- CORRECTED



λ (A)

FIGURE 26
FLUORESCENT SPECTRUM OF
BLOOD SERUM SAMPLE

EXCITING LINE 3600 Å
 SLIT WIDTHS 0.5 MM.
 VOLTS / STAGE 100
 DISL. LEVEL 10 M.V.
 ----- CORRECTED

3) Estrone

99% was dissolved in 2 ml. concentrated sulphuric acid and excited by an ultra-violet band at 3650 Å. The resulting fluorescence consisted of a strong single peak at 4840 Å.

4) Dienoestrol

37.5% in 2 ml. concentrated sulphuric acid fluoresced very weakly when excited by the 3650 band, displaying peaks of intensity at 4500, 4920, 5150 and 6000 angstroms.

5) Male Urine Sample

When excited by an ultra-violet band at 3600 Å, this sample fluoresced very strongly with a single peak at 4300 Å.

6) Blood Serum

The fluorescence of this sample was extremely weak with a double peak, barely resolved by the instrument, having maxima at 4900 and 5100 angstroms. Somewhat greater activity is indicated beyond 6000 angstroms, outside the range of the instrument.

The spectra obtained from the estrogens depend on their reactions with the acid and are indicative of the configuration of the complex molecules so formed. Any possible

analyses of the molecular structure from these curves however, being outside the scope of this paper as well as beyond the ability of the experimenter, is left to the chemist. It should be mentioned that during the period of the reaction, which was in some cases as long as four hours (at room temperature), the spectral distribution and intensity of the fluorescence varied considerably. The spectra illustrated were obtained after stability had presumably been reached. The blood and urine spectra are of little interest unless the liquids are first fractionated, and show only that the fluorescence is strong enough to be analyzed by the instrument.

CONCLUSIONS

The construction of a light measuring device of high sensitivity has been described, its characteristics assessed, and its performance illustrated by its application to the analysis of several organic fluorescent spectra.

While similar results have been obtained by photographic methods, these lack speed and convenience. Similar organic spectra measured in this laboratory with a Hilger Medium Quartz spectrograph required exposure times of from 10 to 30 minutes with a slit width of 1.40 millimeter.⁽¹¹⁾ The plates so obtained then, of course, had to be processed and the spectrum analyzed with a densitometer.

The most serious limitation of the instrument is its narrow spectral range, which, for accurate measurements, is only from 4000 to 6000 angstroms. While it is known that the compounds under consideration display little activity in the ultra-violet region, it is strongly suspected that the spectra may extend into the infra-red. Consequently attempts are being made to obtain photomultipliers whose spectral responses are compatible with these requirements.

Due to the weakness of the activities measured, the upper limit of 40,000 counts per minute imposed on the system by the low scaling factor did not interfere with the measurements. However, the scaler is now being replaced by

a ratemeter, simply for more convenient operation, and some thought is being given to the inclusion in the system of an automatic pen recorder.

It may be concluded that the commercial types of photomultiplier used, when cooled to liquid oxygen temperature, are suitable for application to the measurement of low light levels, but only if carefully selected. This process of selection will yield at the most only one or two good tubes out of ten.

REFERENCES

- 1) P.A. Macdonald and M. S. Margolese, *Fertility and Sterility*,
1, 1, 26 (1950)
- 2) For discussions of photomultiplier design see:
"Photoelectricity and its Applications" Zworykin and Ramberg,
(John Wiley & Sons, 1947) and:
Z. Bay, *Rev. Sci. Inst.* 12, 127 (1941)
- 3) R. W. Engstrom, *J. Opt. Soc. Am.*, 37, 6, 424 (June, 1947)
- 4) *Ibid*, 430
- 5) R. W. Engstrom, *Rev. Sci. Inst.* 18, 587, (1947)
- 6) For a description of these pumps see:
"The Scientific Foundation of Vacuum Technique" S. Dushman
(John Wiley and Sons, 1949)
- 7) A. Blanc-Lapierre and D. Charles, *J. De Phys. et Rad.*,
5, 239 (Oct. 1944)
- 8) I. Langmuir and H. A. Jones, *G. E. Review*, 30, 7, 310 (1929)
- 9) Holladay, *J. Opt. Soc. Am.* 17, 329 (1928)
- 10) These values were obtained from:
"The Measurement of Radiant Energy" W. E. Forsythe
(McGraw-Hill, 1937)
- 11) See J. H. Linford, *Can. Journal of Med. Sciences*, 30, 199
(1952) and J. H. Linford and O. B. Paulson, *Can. Journal of
Med. Sciences*, 30, 213 (1952).